Transcriptomics supports that pleuropodia of insect embryos function in degradation of the serosal cuticle to enable hatching

Authors

Barbora Konopová[1,2,*], Elisa Buchberger[2], Alastair Crisp[3]

[1] Department of Zoology, University of Cambridge, United Kingdom

[2] Department of Developmental Biology, University of Göttingen, Germany

[3] MRC Laboratory of Molecular Biology, Cambridge, United Kingdom

* author for correspondence: barbora.konopova@biologie.uni-goettingen.de

EB: elisa.buchberger@biologie.uni-goettingen.de

AC: acrisp@mrc-lmb.cam.ac.uk

Keywords

insect, Orthoptera, RNA-seq, pleuropodia, embryonic organ, gland, moulting fluid, chitinase, immunity, ecdysone

ABSTRACT

Pleuropodia are limb-derived vesicular organs that transiently appear on the first abdominal segment of embryos from the majority of insect "orders". They are missing in the model *Drosophila* and little is known about them. Experiments carried out on orthopteran insects eighty years ago indicated that the pleuropodia secrete a "hatching enzyme" that at the end of embryogenesis digests the serosal cuticle to enable the larva to hatch. This hypothesis contradicts the view that insect cuticle is digested by enzymes produced by the tissue that deposited it. We studied the development of the pleuropodia in embryos of the locust *Schistocerca gregaria* (Orthoptera) using transmission electron microscopy. RNA-seq was applied to generate a comprehensive embryonic reference transcriptome that was used to study genome-wide gene expression of ten stages of pleuropodia development. We show that the mature and secretion releasing pleuropodia are primarily enriched in transcripts associated with transport functions. They express genes encoding enzymes capable of digesting cuticular protein and chitin. These include the potent cuticulo-lytic Chitinase 5, whose transcript rises just before hatching. The pleuropodia are also enriched in transcripts for immunity-related enzymes, including the Toll signaling pathway, melanization cascade and lysozymes. These data provide transcriptomic evidence that the pleuropodia of orthopterans produce the "hatching enzyme", whose important component is the Chitinase 5. They also indicate that the organs facilitate epithelial immunity and may function in

40 embryonic immune defense. Based on their gene expression the pleuropodia appear

41 to be an essential part of insect physiology.

INTRODUCTION

An integral part of insect embryogenesis is the transient appearance of enigmatic glandular organs on the first abdominal segment (A1) that are called the pleuropodia (Rathke, 1844; Wheeler, 1889) (Figure 1A-C). These are paired structures that form external vesicles in some species while in others they sink down into the body wall (reviewed in e.g., Wheeler, 1889; Hussey, 1926; Roonwall, 1937). The pleuropodia are peculiarly modified limbs (Machida, 1981; Bennett, 1999; Lewis, 2000) (Figure 1D,E): their buds emerge in a line with the buds for the walking legs, but unlike the legs, the pleuropodia remain short, the majority of their cells massively enlarge and develop into a transporting-like and secretory epithelium (Bullière, 1970; Louvet, 1973; Louvet, 1975; Stay, 1977). The pleuropodia degenerate before hatching and are absent in larvae. They have been found in at least some species of nearly all insect "orders" (Figure 1F), but are absent in others, like Diptera, Hymenoptera and advanced Lepidoptera such as silkworms (e.g., Graber, 1889; Hussey, 1926; Hagan, 1931; Roonwall, 1937; Miller, 1940; Ando, 1962; Stanley and Grundmann, 1970; Ando and Haga, 1974; Bedford, 1978; Miyakawa, 1979; Machida, 1981; Norling 1982; Larink, 1983; Louvet, 1983; Kamiya and Ando, 1985; Tanaka et al., 1985; Kobayashi and Ando, 1990; Heming, 1993; Kobayashi et al., 2003; Lambiase et al., 2003; Machida et al., 2004; Rost et al., 2004; Uchifune and Machida, 2005; Tsutsumi and Machida, 2006; Mashimo et al., 2013; Fraulob et al., 2015). Perhaps because the pleuropodia are missing in the genetic model *Drosophila*, they have been neglected in recent decades. Their

function has remained unclear and the genes expressed during their active stages are unknown.

Eighty years ago Eleanor Slifer (Slifer, 1937; 1938) demonstrated that the pleuropodia of grasshoppers (Orthoptera) are necessary for the digestion of the serosal cuticle (SC) before hatching, to enable the larva to get out of the egg. The SC is a chitin and protein-containing sheet structurally similar to the larval or adult cuticles and is produced by the extraembryonic serosa in early embryogenesis (Goltsev et al., 2009; Jacobs et al., 2015). Shortly before hatching the inner layer of the SC (procuticle) disappears. Slifer (Slifer, 1937) showed that when the pleuropodia are removed from the embryos, the SC remains thick and the larva stays arrested in the egg. She proposed that the pleuropodia secrete the "hatching enzyme", a substance likely similar to the cuticle degrading moulting fluid (MF) that is released by the larval epidermis under the old cuticle when the insect is preparing to moult (Reynolds and Samuels, 1996). The exact molecular composition of this "hatching enzyme" is unknown.

The endocrinologists Novak and Zambre (Novak and Zambre, 1974) argued that this would be an unusual way to digest a cuticle. During larval moulting (Nijhout, 1994) the larval epidermal cells deposit a cuticle and subsequently it is the same epidermal cells, not a special gland that secretes the cuticle degrading MF. Therefore they proposed that the SC degrading enzymes would most probably be secreted by the serosa itself. They proposed that the pleuropodia instead secrete the moulting

hormone “ecdysone”, which then stimulates the serosa to secrete the “hatching enzyme”. They also suggested that the pleuropodia reach the peak of their activity in very young embryos during katatrepsis when the serosa is still present (Panfilio, 2008).

In some insects, including locusts, ultrastructural studies (Bullière, 1970; Louvet, 1973; Louvet, 1975; Rost et al., 2004; Viscuso and Sottile, 2008) have indeed shown that the pleuropodia secrete granules similar to the “ecdysial droplets” carrying the MF (Locke and Krishnan, 1973). Some of the Slifer’s experiments (Slifer, 1937) were successfully repeated by others (Jones, 1956) and a substance capable of digesting pieces of SC was even isolated from the pleuropodia (Shutts, 1952). But a proper validation by the state-of-the-art genetic methods that the pleuropodia express genes for enzymes capable to digest the SC is missing.

Here, we identified the mRNAs expressed in the pleuropodia of the locust *Schistocerca gregaria* (Orthoptera). We chose *Schistocerca* as an ideal model, because it has large embryos (eggs over 7 mm) and external pleuropodia that can easily be dissected out, and because the previous experiments testing the function of pleuropodia were carried out in orthopterans. We studied the development of the pleuropodia including using transmission electron microscopy (TEM), and by high-throughput RNA sequencing (RNA-seq) generated transcriptomes from ten morphologically defined stages. We performed differential gene expression analysis between the pleuropodia and similarly aged hind legs. For mapping of reads we

assembled a transcriptome from whole embryos. The goal of this paper was to investigate whether the observed gene expression profile of the pleuropodia is consistent with the idea that these are organs for the secretion of the "hatching enzyme". We show that during their high secretory activity the pleuropodia express genes for cuticle degrading chitinase and proteases that were previously identified in the MF. This supports the "hatching enzyme hypothesis" (Slifer, 1937; 1938).

RESULTS

Development of pleuropodia in the course of *Schistocerca* embryogenesis

Before we could start exploring the genes expressed in the pleuropodia of *Schistocerca* we needed to understand how these organs develop in the locust, when they are fully differentiated and show activity. Cytological study of developing pleuropodia in grasshopper embryos was previously carried out by Slifer (Slifer, 1938), but the light microscopy that she used does not provide sufficient resolution to distinguish the fine ultrastructure of the cells. Ultrastructure of pleuropodia by TEM has been described for several insects (Bullière, 1970; Louvet, 1973; Louvet, 1975; Stay, 1977; Louvet, 1983; Rost et al., 2004; Viscuso and Sottile, 2008), but a chronological study is missing for *Schistocerca* or any other orthopteran.

Under our conditions *Schistocerca* embryogenesis lasts 14.5 days (100% developmental time, DT) (Figure 2A, S1). We followed the development of the

pleuropodia from the age of 4 days (27.6 % DT), when all appendages are similar looking short buds, until just before hatching, day 14 (Figures 2B, S2-S3). Simultaneously, we followed the development of the hind leg, which we used for comparison (because pleuropodia are peculiarly modified legs).

We traced cell divisions in the pleuropodia by using Phosphohistone- 3 as a marker (Figure 2C). The glandular cells were labeled only in the days 4 and 5. From day 6 onwards no cell divisions were detected and the nuclei started to enlarge as the cells became polyploid (Grellet, 1971). The pleuropodial stalk cells, haemocytes entering the pluropodia and cells in the other embryonic tissues kept dividing.

Although the pleuropodia get their final external mushroom-like shape just before the embryos undergo katatrepsis (day 6; 41.4% DT) (Figure 2A,B), we found by TEM (Figure 3) that the glandular cells fully differentiate only later, shortly before dorsal closure (day 8; 55.2% DT) (compare the undifferentiated cells in Figure 3F-I, with differentiated cells in Figure 3J-P). At that time these cells form a single-layered transporting-like epithelium (Berridge and Oschman, 1972) and secretion granules inside and outside the cells become visible (Figure 3A-E, J). The granules outside of the cells first appear at the base and in between the long apical microvilli (brush-border) (Figure 3E,J). The whole pleuropodium is covered with a thin embryonic cuticle ("the first embryonic cuticle", EC1); the tips of the microvilli produce fibrous material that is a part of this cuticle (Figure 3E) (compare with similar fibers above the leg epidermis in Figure S4).

157

158 As development progresses the secretion granules (inside and outside the cells)
159 become more abundant and are present also above the microvilli (Figure 3K-P). On
160 day 12 the apical side of the glandular cells changes: clusters of microvilli (usually at
161 the borders between cells) elevate (Figure 3N). Later the cells show signs of
162 degeneration, the chromatin condenses and the cell content becomes disorganized
163 (Figure 3O,P). Large secretion granules are still abundant and probably released
164 even on the last day before hatching, when the pleuropodia have shrunk and
165 collapsed (Figures 2B,3P).

166

167 When the embryo moults (apolyses a cuticle and secretes a new one), first at about
168 8.5 days and again just before 12 days (Figures 2A, S4), ecdysial droplets are present
169 below the apolysed cuticle. These droplets are very similar at both moults (compare
170 Figures S4F and I). They are very similar, but not identical to the granules released
171 by the pleuropodia (Figure 4A,B). The glandular cells of the pleuropodia do not
172 moult and keep the first embryonic cuticle (EC1) their whole life-time.

173

174 At hatching, the larva enclosed in the (now apolysed) second embryonic cuticle
175 (EC2) leaves the eggshell and digs through the substrate up to the surface (Bernays,
176 1971; Konopova and Zrzavy, 2005). Here the EC2 is shed and the degenerated
177 pleuropodia are removed with it (Roonwall, 1937; Figure 2A).

178

Therefore our observations show that the timing of the high secretory activity corresponds to the stages when Slifer (Slifer, 1937) demonstrated the presence of the "hatching enzyme" (Figure 2A). Next we looked at what genes are expressed in the pleuropodia at this time.

Generation of a comparative RNA-seq dataset from developing pleuropodia and legs of *Schistocerca*

To find out what genes are upregulated in the pleuropodia of *Schistocerca*, we applied a comparative genome wide expression analysis using RNA-seq. We generated a comprehensive embryonic transcriptome (see details in Materials and Methods) that served as reference for the analysis. This transcriptome consists of 20834 transcripts (Table S1). Its completeness was assessed using the open-source software BUSCO (version 3) (Simão et al., 2015; Waterhouse et al., 2018). 95.6%, 96.3% and 94.6% of the Metazoa, Arthropoda and Insecta orthologs, respectively, were found, a level comparable to published "complete" transcriptomes.

To gain insights into the gene expression dynamics of pleuropodia development, we dissected pleuropodia from ten embryonic stages and isolated their mRNAs. In parallel, we dissected hind legs for the same ten stages to generate a comparative transcriptomic dataset. In total we sequenced pairs of samples (pleuropodia and legs) from ten developmental stages and performed a differential expression analysis between legs and pleuropodia for each stage (Figure 2A, Table S2). A

202 principal component analysis (PCA) confirmed that legs and pleuropodia are not
203 only morphologically very similar at early stages, but share a common
204 transcriptomic landscape as well (Figure 5A). The number of differentially
205 expressed genes (DEGs) rises as development progresses (Figure 5B, Table S3).
206
207 For several genes whose expression dynamics in the pleuropodia were already
208 known, such as *Ubx*, *abd-A*, *dll* and *dac* (e.g., Tear et al., 1990; Bennett et al., 1999;
209 Prpic et al., 2001; Hughes and Kaufman, 2002; Angelini et al., 2005; Zhang et al.,
210 2005), we confirmed that they were up- or downregulated in our RNA-seq data as
211 predicted (Table S4). To further validate the RNA-seq dataset, we carried out real-
212 time RT-PCR on 46 selected genes in several stages (in total in 176 cases) and got
213 results consistent with the sequencing data (Table S5). Therefore we are confident
214 that we can identify important factors that are relevant for pleuropodia function and
215 development.
216
217 **Identification of genes upregulated in the intensively secreting pleuropodia**
218
219 Since we wanted to focus specifically on the pleuropodia with high secretory activity
220 we pooled the data from the samples 10, 11 and 12 days together, separately for
221 pleuropodia and legs, and treated them as triplicates. These three samples cover the
222 stages from the embryos after the dorsal closure, when the pleuropodia intensively
223 release secretion granules, but are not in advanced state of degeneration (day 13)
224 (Figures 2A, 3L-N). We performed differential expression analysis and gene

ontology (GO) enrichment analysis with genes upregulated in legs and pleuropodia. We identified 781 transcripts upregulated in the pleuropodia (compared to the legs) and 1535 downregulated (Table S3). Table 1 shows the top ten percent of the most highly abundant transcripts (measured in RPKM units, "reads per kilobase of transcript per million reads mapped") that we found upregulated in the pleuropodia.

For the sake of clarity we summarized redundant GO terms in representative GO-groups (Figure 6; the full set of enriched GO terms are presented in Tables S6, S7; GOs enriched at each developmental stage separately are in Tables S8, S9). Our results show that the genes downregulated in the pleuropodia (upregulated in the legs) are enriched in GO terms associated with development and function of muscle tissue, cell division and DNA synthesis. This is in agreement with our and previous observations that the pleuropodia lack muscles, while at these stages the legs are differentiating, developing muscles and their cells are still dividing (Figure 2C). The pleuropodia downregulate genes for the development of mesoderm, which is consistent with the morphological observation that they are formed by ectodermal cells (Figure 3A).

The upregulated genes are primarily enriched in GO terms (Figure 6, Table S7) associated with transport, thus genetically confirming the morphological observations that the pleuropodia are transporting organs. These include genes for transporters present in typical insect transporting epithelia (Chintapalli et al.,

248 2013), such as the energy providing V-ATPase and Na^+, K^+ ATPase (Table S10). We
249 found enriched GO terms linked with lysosome organization, consistent with the
250 observation that the pleuropodia contain numerous lysosomes (Figure 3, Louvet
251 1975). We also found a large cluster of GO terms associated with lipid metabolism,
252 consistent with the abundant smooth endoplasmic reticulum in the cells. Therefore,
253 the pool of genes expressed in the pleuropodia is in agreement with the morphology
254 of the organs. Among the novel findings are upregulation of genes associated with
255 immunity, as well as with carbohydrate derivative metabolism, aminoglycan
256 catabolic process and proteolysis: these might contain genes for degradation of the
257 SC. Next we looked at selected genes in a detail.
258
259 **Pleuropodia upregulate genes for cuticular chitin degrading enzymes**
260
261 Insect cuticle is digested by a cocktail of chitin and protein degrading enzymes
262 (Reynolds and Samuels, 1996; Zhang et al., 2014). Cuticular chitin is hydrolyzed by a
263 two-enzyme system composed of a β-N-acetyl-hexosaminidase (NAG) and a
264 chitinase (CHT) (Zhu et al., 2016). Both types of enzymes, a NAG and a chitinase,
265 have to be simultaneously present for efficient hydrolysis of chitin (Fukamizo and
266 Kramer, 1985). Previous studies have shown that only particular NAGs and CHTs
267 are capable of efficiently digesting the type of chitin present in the insect cuticle (see
268 below).
269

Insect NAGs were classified into four major classes, of which chitinolytic activity was demonstrated for group I and II (Table 2) (Hogenkamp et al., 2008; Rong et al., 2013). Our transcriptome contains four NAG transcripts, each representing one group (Table 2, Figures 7A-D, S5A, S6A). All were upregulated in the pleuropodia. Among them the *Sg-nag2* for the chitinolitic NAG group II had the highest expression (among 46 most highly "expressed" genes, Table 1) and fold change between legs and pleuropodia. The abundance of transcripts for the chitinolitic NAGs starts to rise from day 6 (Figure 7A,B) when the glandular cells in the pleuropodia begin to differentiate morphologically (Figures 1, 3). The expression profile of *Sg-nag2*, that we have chosen for validation, was similar by RNA-seq and real-time RT-PCR (compare Figure 7B and B').

To see if the pleuropodia are the major source of the *Sg-nag2* transcript in the embryo, we looked at its expression in various parts of the body (head, thorax, abdomen with pleuropodia, abdomen from which pleuropodia were removed) using real-time RT-PCR (Figure 8A,B). We performed this analysis in embryos on day 6, when the pleuropodia are still immature, day 8, just at the onset of the secretory activity, day 10 and day 12 during active secretion. During all of the stages the abdomen with pleuropodia had the highest expression (A+ in Figure 8B), although the expression was lower in the youngest sample (day 6) compared to the samples from older embryos (day 8, 10 and 12). This shows that the pleuropodia are the major source of mRNAs for this cuticle-degrading NAG.

293 The insect CHTs have been classified into several groups (Zhu et al., 2016; Noh et al.,
294 2018), of which the major role in the digestion of cuticular chitin is played by
295 Chitinase 5 and (perhaps with a secondary importance) by Chitinase 10 (Zhu et al.,
296 2008; Qu et al. 2014) (Table 2; the classification of CHTs into five major groups that
297 we use here is based on Zhu et al., 2008). Some chitinases, for example, are
298 expressed in the gut, trachea and fat body, where they are likely involved in
299 digestion of dietary chitin, turnover of peritrophic matrix and immunity, other
300 chitinases expressed by the epidermis organize assembly of the new cuticle (e.g.,
301 Yan et al., 2002; Shi and Paskewitz, 2004; Pesch et al., 2016; Noh et al., 2018).
302
303 Our transcriptome contains 16 full or partial transcripts of CHTs representing all of
304 the major CHT groups (Table 2, Figure S5B, S6B). The pleuropodia specifically
305 upregulate both of the genes for Chitinase 5, homologs of *cht5-1* and *cht5-2* from the
306 locust *Locusta migratoria* (Li et al., 2015). One of the transcripts, *Sg-cht5-1*, was
307 among the top 15 most abundant transcripts upregulated in the highly secreting
308 pleuropodia (Table 1). The predicted amino acid sequence contains a conserved
309 catalytic domain and a signal peptide, and thus is likely to be active and secreted,
310 respectively (Figure S5B). The other upregulated CHTs were homologs of *cht2* and
311 *idgf*. By contrast, the *Schistocerca* homolog of *cht10* that also has a role in cuticular
312 chitin hydrolysis and required for larval moulting (Zhu et al., 2008; Pesch et al.,
313 2016) had low expression in both legs and pleuropodia.
314

We next focused on the transcript of the major chitinase, *Sg-cht5-1*. Unlike the NAGs, both RNA-seq and real-time RT-PCR have shown that the expression of this CHT is low in the early secreting stages, rises only later around day 12 and reaches highest levels when the pleuropodia are already degenerating (day 13 and 14) (Figure 7 F,G,F'). Also real-time RT-PCR on cut embryos has shown that the pleuropodia are a major source of the *Sg-cht5-1* mRNA on day 12 but not before (the high expression in the whole embryo on day 10 could be linked to the second embryonic moult and was also observed with *Sg-cht7*, although not with *Sg-cht10*, Figure S8). These data show that the pleuropodia before hatching express a cuticle-degrading chitinase.

Pleuropodia upregulate transcripts for some proteases that could digest a cuticle

Our GO enrichment analysis has shown that the secreting pleuropodia are enriched in transcripts for genes associated with proteolysis (Figure 6, Table S11). Transcripts for proteases and their inhibitors are abundant among the top ten percent of the most highly "expressed" upregulated DEGs (Table 1). To see if the upregulated transcripts encode enzymes that are associated with digestion of insect cuticle, we compared our data with the enzymes identified in the complete proteomic analysis of the MF from the lepidopteran *Bombyx mori* (Zhang et al., 2014; Liu et al., 2018). Out of 69 genes that we searched, we found homologs or very similar genes in *Schistocerca* transcriptome for half of them (35). This made in total 75 transcripts, of which 27 were upregulated (seven among the top ten percent

most highly expressed) and 15 downregulated (Tables 3, S12). The prominent MF protease Carboxypeptidase A (Sui et al., 2009; Zhang et al., 2014) and the Trypsin-like serine protease known to function in locust moulting (Wei et al., 2007) were not upregulated in the pleuropodia. These data indicate that the pleuropodia upregulate transcripts for proteolytic enzymes associated with the degradation of the cuticle and would be able to contribute to the digestion the SC, although the enzymatic cocktail produced by the pleuropodia may not be identical with the MF.

Pleuropodia are enriched in transcripts for immunity-related proteins

An observation that was not anticipated was the upregulation of genes for proteins involved in immunity (Lemaitre and Hoffmann, 2007; Buchon et al., 2014) (Figures 6, 9, Table S13). This is especially interesting, because immunity related proteins have been found in the MF (Zhang et al., 2014). This is in agreement with that the cells in the pleuropodia are a type of barrier epithelium (Lemaitre and Hoffmann, 2007; Buchon et al., 2014; Bergman et al., 2017), which enables the contact between the organism and its environment. Barrier epithelia (e.g., the gut, Malpighian tubules or tracheae) constitutively express genes for immune defense.

In total we found upregulated 99 transcripts (13 percent of the upregulated genes) for immunity-related proteins. These include proteins at all three levels, the pathogen recognition, signaling and response (Figure 9, Table S13). From the four signaling pathways, Toll was upregulated, but not IMD or JAK/STAT, and from the

361 JNK signaling we found c-Jun. Genes for a range of immune responses were
362 upregulated, including production of reactive nitrogen species (RNS), melanization,
363 genes for lysozymes and one antimicrobial peptide (AMP) similar to Diptericin.
364
365 The transcripts for lysozymes were among the most highly expressed (Table 1) and
366 we chose to focus on them. Lysozymes are secreted proteins that kill bacteria by
367 breaking down their cell wall. Our *Schistocerca* transcriptome contains nine genes
368 for lysozymes, seven of which were upregulated (Table 4, Table S14). The second
369 most highly expressed DEG was a transcript for a C-type lysozyme *(Sg-LyzC-1)* that
370 was previously shown to have anti-bacterial properties in *Schistocerca* (Mohamed et
371 al., 2016) (Table 1). We examined expression of five selected genes on cut embryos
372 by real-time RT-PCR (Figure 9). Our data showed that the pleuropodia are the major
373 source of mRNAs for these genes.
374
375 **Pleuropodia do not upregulate the pathway for ecdysone biosynthesis**
376
377 Previous work has suggested that pleuropodia may be embryonic organs producing
378 the moulting hormone ecdysone (Novak and Zambre, 1974). During post-embryonic
379 stages, ecdysone is synthesized in the prothoracic glands and several other tissues
380 by a common set of enzymes (reviewed in Niwa and Niwa 2014; Ou et al., 2016),
381 some which have been characterized in the locusts (Marchal et al., 2011, 2012;
382 Lenaerts et al., 2016; Sugahara et al., 2017). As shown in *Drosophila*, these genes are
383 expressed in diverse cell types in embryos, and when the larval prothoracic glands

384 are formed their expression co-localizes there (Chávez et al., 2000; Warren et al.,
385 2002; Petryk et al., 2003; Niwa et al., 2004; Warren et al., 2004).
386
387 Out of the nine genes critical for ecdysone biosynthesis, only one (*dib*) was
388 upregulated in the highly secreting pleuropodia (Table 5, S15). One gene (*spo*) was
389 downregulated. The pleuropodia are not enriched in the whole pathway at any time
390 of development, including around katatrepsis, in which experiments supporting the
391 synthesis of moulting hormone were carried out (Table S9, S16). Under the GO term
392 "hormone biosynthetic process" enriched in the highly secreting pleuropodia (Table
393 S7, S17) we found a gene *Npc2*a that encodes a transporter of sterols including
394 precursors of ecdysone. It is also required for ecdysone biosynthesis, but indirectly
395 and in the cells it functions as a general regulator of sterol homeostasis (Huang et al.,
396 2007). We conclude that our transcriptomic data provide little evidence that the
397 pleuropodia are involved in ecdysone biosynthesis.
398
399 **DISCUSSION**
400
401 **Pleuropodia of *Schistocerca* express genes for the "hatching enzyme"**
402
403 The first demonstration of the physiological role of the pleuropodia comes from the
404 experiments carried out on a grasshopper *Melanoplus* (closely related to
405 *Schistocerca*), by Eleanor Slifer (Slifer, 1937). When she took embryos before
406 hatching (Figure 2) and separated anterior and posterior halves by ligation, the SC

was digested only in the part of the egg with the pleuropodia. Surgical removal of the pleuropodia prevented SC digestion in the whole egg. Slifer's hypothesis that the pleuropodia secrete the "hatching enzyme" was criticized by Novak and Zambre (1974): if the deposition and digestion of the SC is similar to the cuticle turnover during larval moulting, then the "hatching enzyme" is produced by the serosa. They believed that the pleuropodia reach the peak of their activity in embryos during katatrepsis (45% DT) and participate in digestion of the SC indirectly by secreting ecdysone to stimulate the serosa.

Our ultrastructural observations on staged pleuropodia of *Schistocerca* have shown that the glandular cells only begin to differentiate just at the time of katatrepsis (45% DT) and do not secrete at that time. This would explain why no digestive effect on the SC was detected by Novak and Zambre (Novak and Zambre, 1974) using a homogenate from *Schistocerca* pleuropodia isolated at this stage. The release of granular secretion starts just before dorsal closure (55% DT) and intensifies before hatching. This is in agreement with previous observations on some stages of the pleuropodia in other orthopterans (Louvet, 1975; Viscuso and Sottile, 2008).

Our RNA-seq analysis revealed that the secreting pleuropodia highly express genes encoding enzymes that are capable of digesting a typical chitin-protein insect cuticle. These include genes for proteolytic enzymes similar to those present in the MF and cuticular chitin-degrading NAGs and Chitinase 5. The pleuropodia also express genes for Chitinase 2 and Idgf, which have low effect on cuticular chitin

digestion, but were shown to organize proteins and chitin fibres during cuticle deposition (Pesch et al., 2016). These CHTs may organize the fibres in the cuticle secreted by the pleuropodia (Figure 3).

In combination with RT-PCR we showed that, while the expression of the *Sg-nag1* and *Sg-nag2* started to rise in parallel with the differentiation of the glandular cells, the *Sg-cht5-1* and *Sg-cht5-2* transcripts raised shortly before hatching. Chitinase 5 is a critical chitin-degrading chitinase in insects: it is highly abundant in the moulting fluid and its silencing in diverse insects including locusts leads to failure in larval moulting (Zhu et al., 2008; Zhang et al., 2014; Li et al., 2015; Xi et al., 2015; Pesch et al., 2016). Our data indicate that the sudden rise in the expression of *Sg-cht5* in the pleuropodia at the end of embryogenesis and presumably secretion of this CHT into the extraembryonic space is the key component of the "hatching enzyme" effect (Slifer 1937; 1938) in locusts and grasshoppers.

Pleuropodia in some other insects could secrete the "hatching enzyme" and their function may also vary among species

There is evidence to suggest that the process occurs similarly in some insect. As in orthopterans, the pleuropodia of the rhagophthalmid beetle *Rhagophthalmus ohbai* release secretion after katatrepsis and SC rapidly degrades just shortly before hatching (Kobayashi et al., 2003). In the large water true bugs from the family Belostomatidae, the male carries a batch of eggs on his back. It is believed that the

453 detachment of the eggs just before hatching is also caused by the secretion from the
454 pleuropodia (Tanizawa et al., 2007).
455
456 The molecular mechanism of SC degradation may also vary between insects and as
457 previously hypothesized (Novak and Zambre, 1974) the serosa may also contribute
458 to the SC degradation. The serosa of the beetle *Tribolium*, expresses *cht10* and *cht7*
459 (Jacobs et al., 2015), of which the former CHT is important for cuticular chitin
460 digestion. Silencing of *cht10*, but not *cht5* prevented larvae from hatching (Zhu et al.,
461 2008). Transcripts for *cht10* were not upregulated in the pleuropodia of
462 *Schistocerca*. This suggests that the SC is degraded by enzymes produced by both,
463 the serosa and the pleuropodia and that the indispensable roles in cuticle digestion
464 are played by different enzymes in different insects.
465
466 In some insects the pleuropodia may not be involved in hatching but have another
467 function. In the viviparous cockroach *Diploptera punctata* (Stay, 1977), the secretion
468 from the pleuropodia is very low and the large pleuropodia of the melolonthid
469 beetle *Rhizotrogus majalis* have not been observed to produce any secretion
470 granules at all (Louvet, 1983). In dragonflies, one of the more basal lineages of
471 insects, the secretion likely has a different function than in orthopterans, because
472 their SC is not digested before hatching (Ando, 1962). The special epithelium in the
473 pleuropodia shares features with transporting epithelia (Louvet, 1973; Stay, 1977)
474 that function in water transport and ion balance (Berridge and Oschman, 1972). Our
475 data do not exclude this function, but it is yet to be tested.

476

477 **The pleuropodia of *Schistocerca* are enriched in transcripts for enzymes**

478 **functioning in immunity**

479

480 We found that many of the genes expressed in the pleuropodia encode proteins

481 involved in immunity (Lemaitre and Hoffmann, 2007). This indicates that the

482 pleuropodia are also organs of epithelial immunity, similar to other barrier epithelia

483 in postembryonic stages (such as the gut) (Bergman et al., 2017), which are in a

484 constant contact with microorganisms. The pleuropodia differ from such tissues in

485 that they are not directly exposed to the environment, but enclosed in the eggshell,

486 seemingly limiting their contact with microorganisms. Proteins associated with

487 immune defense are also found in the MF (Zhang et al., 2014), where they prevent

488 invasion of pathogens through a "naked" epidermis after the separation of the old

489 cuticle from the epidermis in the process of apolysis. As found in the beetle

490 *Tribolium*, during the early embryonic stages the frontier epithelium providing the

491 egg with an immune defense is the extraembryonic serosa (Jacobs et al., 2014). The

492 serosa starts to degenerate after katatrepsis and disappears at dorsal closure

493 (Panfilio, 2008). The pleuropodia of *Schistocerca* differentiate just before dorsal

494 closure, suggesting that they take over this defense function in late embryogenesis.

495 It will be interesting to clarify in the upcoming research whether apart from their

496 role in hatching the pleuropodia are important organs for fighting against potential

497 pathogens that have gained access to the space between the embryo and the

498 eggshell.

Conclusions

The pleuropodia of *Schistocerca* have morphological markers of high secretory activity in the second half of embryogenesis after the definitive dorsal closure is finished. Transcriptomic profiling indicate that the conclusions that Eleanor Slifer drew from her experiments over eighty years ago that the pleuropodia secrete cuticle degrading enzymes, were correct. The pleuropodia likely have other functions, such as in immunity. The pleuropodia are specialized embryonic organs and apparently an important though neglected part of insect physiology.

MATERIALS AND METHODS

Insects

Schistocerca gregaria (gregarious phase) were obtained from a long-term, partly inbred colony at the Department of Zoology, University of Cambridge. Eggs were collected into aluminium pots filled with damp sand. The pots were picked up after two (most samples) or four hours and incubated at 30°C.

Description of embryonic stages

Embryos and appendages were dissected in phosphate buffer saline (PBS). Whole eggs were bleached in 50% household bleach to dissolve the chorion. All were photographed in water or PBS using the Leica M125 stereomicroscope equipped with DFC495 camera and associated software. Photos were processed using Adobe Photoshop CC 2017.1.1. Photos of eggs and embryos that illustrate the stage (Figure 2A and S1) had the background cleaned using the software (removal of the tools that hold the photographed objects in place).

Immunohistochemistry on paraffin sections

Embryos were dissected in PBS and pieces including posterior thorax and anterior abdomen (older embryos) or mid thorax plus whole abdomen (young embryos) were fixed in PEMFA (4% formaldehyde in PEM buffer: 100 mM PIPES, 2.0 mM EGTA, 1.0 mM $MgSO_4$) at room temperature (RT) for 15-30 minutes, then washed in PBT (PBS with 0.1% Triton-X 100) and stored in ethanol at -20°C.
Samples were cleared in 3x10 minutes in Histosol (National Diagnostics) at RT, infiltrated with paraffin at 60°C for 2-3 days, embedded in moulds and hardened at RT. Sections 6-8 µm thick were prepared on a Leica RM2125RTF microtome. The slides with sections were washed with Histosol, ethanol, then stepwise re-hydrated to PBT. Incubations were carried out in a humidified chamber. Slides were blocked with 10% sheep serum (Sigma-Aldrich) in PBT for 30 minutes at RT, incubated with Phospho-Histone H3 antibody (Invitrogen) diluted with PBT 1:130 at 4°C overnight, washed and incubated with Alexa Fluor 568 anti-rabbit secondary antibody

(Invitrogen) diluted 1:300 at RT for 2 hours, washed and incubated with DAPI (Invitrogen) diluted 1:1000. Sections were imaged with a Leica TCS SP5 confocal microscope and photos processed using Fiji (https://fiji.sc).

Electron microscopy

For TEM embryos were removed from the chorion in PBS and pieces of posterior thorax to anterior abdomen were fixed in 2.5-3.0% glutaraldehyde in 0.1 M phosphate buffer pH7.2 for a few hours at room temperature and then at 4°C for several days. Each pleuropodium and leg were then separated and embedded into 2% agar. Small cubes of agar with the tissue were incubated in osmium ferrocyanide solution (3% potassium ferricyanide in cacodylate buffer with 4 mM calcium chloride) for 1-2 days at 4°C, then in thiocarbohydrazide solution (0.1 mg thiocarbohydrazide from Sigma-Aldrich, and 10 ml deionized water dissolved at 60°C) and protected from light for 20-30 minutes at RT, then in 2% aqueous osmium tetroxide 30-45 minutes at RT and in 1% uranyl acetate (maleate buffered to pH 5.5) at 4°C overnight. Washing between each step was done with deionized water. Samples were dehydrated in ethanol, washed with dry acetone, dry acetonitrile, infiltrated with Quetol 651 resin (Agar Scientific) for 4-6 days and hardened in moulds at 60°C for 2-3 days. Semithin sections were stained with toluidine blue. Ultrathin sections were examined in the Tecnai G280 microscope.

For SEM whole embryos were dissected out of the chorion in PBS, fixed in 3% glutaraldehyde in phosphate buffer similarly as above. They were post-fixed with osmium tetroxide, dehydrated through the ethanol series, critical point dried, gold coated, and observed in a FEI/Philips XL30 FEGSEM microscope. Photos from TEM and SEM were processed using Adobe Photoshop CC 2017.1.1.

Preparation of the reference transcriptome

Whole embryo transcriptome: Eggs from each 1-day egg collection incubated for the desired time were briefly treated with 50% bleach, washed in distilled water and frozen in liquid nitrogen. Total RNA was isolated with TRIzol reagent (Invitrogen), treated with TURBO DNase (Invitrogen) and purified on a column supplied with the RNAeasy Kit (Quiagen). The purified RNA from each day (14 samples) was pooled into 4 samples: day 1-4, 5-7, 8-10 and 11-14. Ten µg of RNA from each of the 4 samples was sent to BGI (Hong Kong). The total RNA was enriched in mRNA by using the oligo(dT) magnetic beads and cDNA library was prepared. 100 bp paired-end (PE) reads were sequenced on Illumina HiSeq 2000; numbers of the reads obtained are in Table S2. Non-clean reads were filtered using filter_fq software (removes reads with adaptors, reads with unknown nucleotides larger than 5% and low quality reads). Transcripts from all samples were assembled separately using the Trinity software (release 20130225) (Grabherr et al., 2011) with parameters: --seqType fq --min_contig_length 100; --min_glue 4 --group_pairs_distance 250; --path_reinforcement_distance 95 --min_kmer_cov 4. Transcriptes from the 4

589 assemblies were then merged together to form a single set of non-redundant
590 transcripts using TGICL software (v2.1) (Pertea, 2003) with parameters: -l 40 -c 10 -
591 v 20.
592
593 Legs and pleuropodia transcriptome (age about 8.5-8.75 days): The appendages
594 were dissected in cold RNase-free PBS (treated with diethyl pyrocarbonate) and
595 total RNA was isolated and cleaned as described above. Ten µg of RNA from each leg
596 sample and pleuropodium sample were transported to the Eastern Sequence and
597 Informatics Hub (EASIH), Cambridge (UK). cDNA libraries were prepared including
598 mRNA enrichment. 75 bp PE reads were sequenced on Illumina GAIIX; numbers of
599 the reads obtained are in Table S2. The reads were trimmed to the longest
600 contiguous read segment for which the quality score at each base is greater than a
601 Phred quality score of Q = 13 (or 0.05 probability of error) using the program
602 DynamicTrim (v. 1.7) from the package SolexQA (Cox et al., 2010;
603 http://solexaqa.sourceforge.net/). The trimmed reads were then filtered to remove
604 sequence adapter using the program cutadapt (v. 0.9;
605 http://code.google.com/p/cutadapt/). Sequences shorter than 40 bp were
606 discarded. Trimmed reads were used to de novo assemble the transcriptome using
607 Velvet (v. 1.1.07; Zerbino et al., 2008; http://www.ebi.ac.uk/~zerbino/velvet/)
608 (commands: -shortPaired –fastq; -short2 –fastq; -read_trkg yes) and Oases (v.
609 0.2.01; Schulz et al., 2012; http://www.ebi.ac.uk/~zerbino/oases/) (commands: -
610 ins_length 350). Velvet is primarily used for de-novo genome assembly; here, the
611 contigs that were output by Velvet were used by the complementary software

612 package Oases to build likely transcripts from the RNA-seq dataset. K-mer sizes of
613 21, 25 and 31 were attempted for the two separate samples as well as the combined
614 samples and optimal K-mer sizes of 21 were found for both samples.
615
616 Transcripts for the reference transcriptome were selected from the embryonic and
617 legs and pleuropodia transcriptomes. The transcripts were first merged with
618 evigene (version 2013.03.11) using default parameters. Because this selection of
619 transcripts eliminated some genes (gene represented by zero transcripts, although
620 the transcripts were present in the original transcriptomes), we repeated the step
621 with less strict parameters (cd-hit-est - version 4.6, with -c 0.80 -n 5). This second
622 selection contained several genes represented by more transcripts, therefore we
623 aligned selection 1 and 2 to each other to identify, which genes in selection 1 were
624 missing. Selection 1 was then completed with the help of selection 2 by adding the
625 missing transcripts. The quality and completeness of the resulting transcriptome
626 was assessed and edited in the following steps. First, we removed several redundant
627 transcripts manually: these were found by blasting diverse insect sequences
628 (queries) against the *Schistocerca* transcriptome using the local ViroBLAST interface
629 (Deng et al., 2007). Some transcripts were edited manually, such as when we found
630 that two transcripts were combined into one, resulting in an alignment against two
631 protein sequences (*Schistocerca* transcript blasted against NCBI GenBank database)
632 we split the respective transcripts. Second, we blasted the whole transcriptome
633 against itself and removed redundant sequences, if the alignment was spanning at
634 least 300 bp with a sequence identity of at least 98% (Blast+ suite, version 2.6.0).

635 The longer transcript was kept in all cases. Transcripts shorter than 200 bp were
636 discarded. All these steps were carried out in R (R Development Core Team, 2008;
637 http://www.R-project.org) and sequences were handled using the Biostrings
638 package (Pagès et al., 2017).
639
640 **Sequence analysis**
641
642 Basic transcript analysis was done by CLC Sequence Viewer7 (QIAGEN). Signal
643 peptide and transmembrane regions were predicted by Phobius (Käll et al., 2007;
644 http://phobius.binf.ku.dk/index.html). Conserved domains were identified using
645 SMART (http://smart.embl-heidelberg.de/). To annotate the newly assembled
646 transcriptome, the freely available annotation pipeline Trinotate (version 3.1.1) was
647 used (Haas et al., 2013). The longest candidate ORF of each sequence was identified
648 with the help of the inbuilt TransDecoder (Haas et al., 2013;
649 https://github.com/TransDecoder/TransDecoder/wiki) software.
650
651 A blast was run against Uniprot sequences specific for *Schistocerca gregaria, Locusta*
652 *migratoria, Apis melifera, Tribolium castaneum, Bombyx mori* and *Drosophila*
653 *melanogaster* (blastx with default parameter and -max_target_seqs 1).
654
655 **RNA-seq expression analysis**
656

Pleuropodia and hind legs from embryos at the same age (day 4, 5, 6, 7, 8, 10, 11, 12 and 13) were dissected in cold RNase-free PBS and total RNA was isolated as described for samples for the reference transcriptome, but cleaned with RNA Clean & Concentrator (Zymo Research). One µg of RNA from each sample was sent to BGI (Hong Kong). The mRNA enrichment and cDNAs preparation was as described above. 50 bp single-end (SE) reads were sequenced on Illumina HiSeq 2000. Over 45 million reads were sequenced from each sample (Table S2).

A pair of samples from mixed embryos 8-9 days that was used for the preparation of the reference transcriptome (described above) was also included in the expression analysis, but prior to mapping, the 75 bp PE reads were trimmed to 50 bp, using Trimmomatic in the paired-end mode (version 0.36) using the CROP function (CROP:50). A single pleuropodium or leg sample was sequenced from each stage.

The quality of the sequenced reads was assessed using the FastQC software. All samples consistently showed a Per base sequence quality of > 30. Reads were mapped to the reference transcriptome with Bowtie2 (version 2.2.5) using default parameter and the –local alignment mode (Langmead et al., 2009). The trimmed pairs of reads were concatenated for each stage and treated as single reads. A PCA plot was generated to assess if differences in sequencing type and processing (SE samples and PE samples day 8-9) had an effect, which was not the case. This plot was prepared by using the plotPCA() function in the DESeq2 R package (Love et al., 2014); the count matrix was transformed with the rlog() function. The R package

HTSFilter (Rau et al., 2013) was used with default parameters to filter constantly low expressed genes and 12988 transcripts were left.

The differential expression analysis was performed with the NOISeq R package (2.22.1; Tarazona et al., 2011). Reads were first normalized using the RPKM method (Mortazavi et al., 2008). We used NOISeq-sim to find the differentially expressed genes between legs and pleuropodium for each stage with the following parameters: k = NULL, norm ="n", pnr =0.2, nss =5, v = 0.02, lc=1, replicates ="no", following the recommendations by the authors for simulation of "technical replicates" prior to differential expression analysis without replicates. Additionally differentially expressed genes between highly secreting pleuropodia and legs at the same stage were assessed (treating samples from day 10, 11 and 12 as replicates) using the NOISeq-real algorithm with the following parameters: k=0.5, norm="n", factor="type", nss=0, lc=1, replicates = "technical". To define significantly differentially expressed genes, the probability ("prob") threshold was set at 0.7 for single stage comparisons and 0.8 for the triplicated comparison, RPKM > 10 and fold change > 2 for both single stage and triplicated comparisons (based on the expression of the genes whose expression dynamics in the pleuropodia were already known, Table S4).

GO enrichment

The transcriptome was blasted against the whole UniProt/Swiss-Prot database to assess the corresponding GO terms. Only blast hits with an e-value <= 1e-5 were considered for the subsequent GO annotation. GO enrichment of differentially expressed genes was performed using the R package GOSeq (version 1:30.0, Young et al., 2010) implemented in the Trinotate pipeline (see above). Enriched GO terms were summarized and visualized with REVIGO (Supek et al., 2011). Dot plots were prepared from DEGs selected at thresholds: RPKM > 50, fold change > 3.

Real-time RT-PCR

Tissues were dissected, total RNA was isolated and DNase treated the same way as for sequencing and cleaned with RNA Clean & Concentrator (Zymo Research). cDNA was synthesized with oligo-dT primer (Invitrogen) and 0.5 µg (legs, pleuropodia) or 1 µg (pieces of embryos) of the RNA using ThermoScript RT-PCR System (Invitrogen) at 55°C. The cDNA was diluted to concentration 40 ng/µl and 5 µl was used in a reaction containing 10 µl of SYBR Green PCR Master Mix (Applied Biosystems) and 5 µl of a 1:1 mix of forward and reverse primers (each 20 nM in this mix). Reactions were run in the LightCycler480 (Roche) and analyzed using the associated software (release 1.5.0 SP1) according to the comparative Ct method and normalized to the *eEF1α* gene. Primers (Table S18) were designed with Primer3PLUS program (Untergasser et al., 2007). To check for the presence of a single PCR product, the melting curve was examined after each run

and for each pair of primers at least 2 finished runs were visualized on a 2% agarose gel.

The program was: denaturation: 95°C for 10 minutes (1 cycle), amplification: 95°C for 10 seconds, 60°C for 15 seconds, 72°C for 12 seconds (40 cycles) melting: 95°C for 5 seconds, 60°C for 1 minute, 95°C.

LIST OF ABBREVIATIONS

A1: first abdominal segment; CHT: chitinase, DEG: differentially expressed gene; DT: developmental time; EC1, EC2, EC3: the first, the second, the third embryonic cuticle, respectively; GO: gene ontology; LEG: hind leg(s); MF: moulting fluid; NAG: β-N-acetyl-hexosaminidase; PCA: principal component analysis; PLP: pleuropodium (pleuropodia); RPKM: reads per kilobase of transcript per million reads mapped; SC: serosal cuticle; SEM: scanning electron microscopy; T3: third thoracic segment; TEM: transmission electron microscopy

COMPETING INTERESTS

The authors declare that they have no competing interests.

FUNDING

This work was supported by Human Frontier Science Program (Long-Term postdoctoral fellowship LT000733/2009-L), Biotechnology and Biological Sciences Research Council (grant number grant BB/ K009133/1), Isaac Newton Trust (University of Cambridge) and Balfour-Browne Fund (University of Cambridge).

AUTHOR'S CONTRIBUTIONS

BK initiated the study, designed research, carried out all experimental work, supervised the bioinformatics analysis, interpreted the data and wrote the paper; EB performed majority of the bioinformatics analysis and edited the draft; AC carried out the initial steps in the selections of transcripts for the reference transcriptome and did a preliminary expression analysis. All authors read and approved the manuscript.

ACKNOWLEDGEMENTS

Majority of the work was carried out in the lab of Michael Akam (University of Cambridge) and the data analysis was finished in the lab of Gregor Bucher (University of Göttingen); BK thanks to both for hosting and financial support. Electron microscopy was done at the Cambridge Advanced Imaging Centre (University of Cambridge). Immunolabeling was done in the lab and with help of Andrew Gillis. Stereomicroscopic pictures were taken in the lab of Paul Brakefield. We also thank for help and advice to Ken Siggens, Jenny Barna, Jeremy Skepper and

770 lab, Steven Van Belleghem, Barry Denholm, Jan Sobotnik, and Gareth Griffiths, for
771 scripts to Erik Clark and Simon Martin. We thank to Michael Akam, Siegfried Roth,
772 Stuart Reynolds, Nico Posnien and Maurijn van der Zee for comments on the
773 manuscript.

774 **REFERENCES**

775

776 Ando H. 1962. The comparative embryology of Odonata with special reference to a
777 relic dragonfly Epiophlebia superstes Selys. Sugadaira Biological Laboratory of
778 Tokyo Kyoiku University.

779

780 Ando H, Haga K. 1974. Studies on the Pleuropodia of Embioptera, Thysanoptera, and
781 Mecoptera. Tokyo U. Educ. Sugadaira Biol. Lab. Bull 6:1-8.

782

783 Angelini DR, Liu PZ, Hughes CL, Kaufman TC. 2005. Hox gene function and
784 interaction in the milkweed bug Oncopeltus fasciatus (Hemiptera). Dev Biol
785 287:440-455.

786

787 Bedford GO. 1978. The development of the egg of Didymuria violescens
788 (Phasmatodea: Phasmatidae: Podacanthinae) – embryology and determination of
789 the stage at which first diapause occurs. Aust J Zool 18:155-169.

790

791 Bennett RL, Brown SJ, Denell RE. 1999. Molecular and genetic analysis of the
792 Tribolium Ultrabithorax ortholog, Ultrathorax. Dev Genes Evol 209:608-619.

793

794 Bergman P, Seyedoleslami Esfahani S, Engström Y. 2017. Drosophila as a Model for
795 Human Diseases-Focus on Innate Immunity in Barrier Epithelia. Curr Top Dev Biol
796 121:29-81.

Bernays EA. 1971. The vermiform larva of *Schistocerca gregaria* (Forskål): form and activity (Insecta, Orthoptera). Z Morph Tiere 70:183–200.

Berridge MJ, Oschman JL. 1972. Transporting epithelia. Academic Press, New York.

Buchon N, Silverman N, Cherry S. 2014. Immunity in Drosophila melanogaster – from microbial recognition to whole-organism physiology. Nat Rev Immunol 14:796-810.

Bullière F. 1970. L'évolution des pleuropodes au cours du développement embryonnaire de la Blabera craniifer (Insecte Dictyoptère). Arch Anat Microsc 59:201-220.

Chávez VM, Marqués G, Delbecque JP, Kobayashi K, Hollingsworth M, Burr J, Natzle JE, O'Connor MB. 2000. The Drosophila disembodied gene controls late embryonic morphogenesis and codes for a cytochrome P450 enzyme that regulates embryonic ecdysone levels. Development 127:4115-4126.

Chintapalli VR, Wang J, Herzyk P, Davies SA, Dow JA. 2013. Data-mining the FlyAtlas online resource to identify core functional motifs across transporting epithelia. BMC Genomics 14:518.

820 Cox MP, Peterson DA, Biggs PJ. 2010. SolexaQA: At-a-glance quality assessment of
821 Illumina second-generation sequencing data. BMC Bioinformatics 11:485.
822
823 Deng W, Nickle DC, Learn GH, Maust B, Mullins JI. 2007. ViroBLAST: a stand-alone
824 BLAST web server for flexible queries of multiple databases and user's datasets.
825 Bioinformatics 23:2334-2336.
826
827 Fraulob M, Beutel RG, Machida R, Pohl H. 2015. The embryonic development of
828 Stylops ovinae (Strepsiptera, Stylopidae) with emphasis on external morphology.
829 Arthropod Struct Dev 44:42-68.
830
831 Fukamizo T, Kramer KJ. 1985. Mechanism of chitin oligosaccharide hydrolysis by the
832 binary enzyme chitinase system in insect moulting fluid. Insect Biochem 15:1-7.
833
834 Goltsev Y, Rezende GL, Vranizan K, Lanzaro G, Valle D, Levine M. 2009.
835 Developmental and evolutionary basis for drought tolerance of the Anopheles
836 gambiae embryo. Dev Biol 330:462-470.
837
838 Graber V. 1889. Ueber den Bau und die phylogenetische Bedeutung der
839 embryonalen Bauchänhange der Insekten. Biol Zent Bl 9:355-363.
840
841 Grabherr MG, Haas BJ, Yassour M, Levin JZ, Thompson DA, Amit I, Adiconis X, Fan L,
842 Raychowdhury R, Zeng Q, Chen Z, Mauceli E, Hacohen N, Gnirke A, Rhind N, di Palma

F, Birren BW, Nusbaum C, Lindblad-Toh K, Friedman N, Regev A. 2011. Full-length transcriptome assembly from RNA-Seq data without a reference genome. Nat Biotechnol 29:644-652.

Grellet P. 1971. Variations du volume et teneur en AND des noyaux de Scapsipedus marginatus Afz. et Br. (Orthoptère, Gryllidae) au cours de l'embryogenèse. Wilhelm Roux Arch Entwickl Mech Mech Org, 167:243-265.

Haas BJ, Papanicolaou A, Yassour M, Grabherr M, Blood PD, Bowden J, Couger MB, Eccles D, Li B, Lieber M, MacManes MD, Ott M, Orvis J, Pochet N, Strozzi F, Weeks N, Westerman R, William T, Dewey CN, Henschel R, LeDuc RD, Friedman N, Regev A. 2013. De novo transcript sequence reconstruction from RNA-seq using the Trinity platform for reference generation and analysis. Nat Protoc 8:1494-1512.

Hagan HR. 1931. The embryogeny of the polyctenid, Hesperoctenes fumarius Westwood, with the reference to viviparity in insects. J Morphol Physiol 51:3-115.

Heming BS. 1993. Origin and fate of pleuropodia in embryos of Neoheegeria verbasci (Osborn) (Thysanoptera: Phlaeothripidae). In: Bhatti JS, editor. Advances in Thysanopterology. New Delhi: Sciantia Publishing. Journal of Pure and Applied Zoology 4. p 205-223.

865 Hogenkamp DG, Arakane Y, Kramer KJ, Muthukrishnan S, Beeman RW. 2008.
866 Characterisation and expression of β-N-acetylhexosaminidase gene family of
867 Tribolium castaneum. Insect Biochem Mol Biol 38:478-489.
868
869 Huang X, Warren JT, Buchanan J, Gilbert LI, Scott MP. 2007. Drosophila Niemann-
870 Pick type C-2 genes control sterol homeostasis and steroid biosynthesis: a model of
871 human neurodegenerative disease. Development 134:3733-3742.
872
873 Hughes CL, Kaufman TC. 2002. Hox genes and the evolution of the arthropod body
874 plan. Evol Dev 4:459-99.
875
876 Hussey PB. 1926. Studies on the Pleuropodia of Belostoma Flumineum Say and
877 Ranatra Fusca Palisot de Beauvois, with a discussion of these organs in other insects.
878 Entomol Am 7:1-82.
879
880 Jacobs CG, Spaink HP, van der Zee M. 2014. The extraembryonic serosa is a frontier
881 epithelium providing the insect egg with a full-range innate immune response. eLife
882 3:e04111.
883
884 Jacobs CGC, Braak N, Lamers GEM, van der Zee M. 2015. Elucidation of the serosal
885 cuticle machinery in the beetle Tribolium by RNA sequencing and functional
886 analysis of Knickkopf1, Retroactive and Laccase2. Insect Biochem Mol Biol 60:7-12.
887

888 Jones B. 1956. Endocrine activity during insect embryogenesis. Control of events in
889 development following the embryonic moult (Locusta migratoria and Locustana
890 pardalina, Orthoptera). J Exp Biol 33:685-696.
891
892 Käll L, Krogh A and Sonnhammer ELL. 2007. Advantages of combined
893 transmembrane topology and signal peptide prediction-the Phobius web server.
894 Nucleic Acids Res 35:W429-432.
895
896 Kamiya A, Ando H. 1985. External morphogenesis of the embryo of Ascalaphus
897 ramburi (Neuroptera, Ascalaphidae). In: Recent Advances in Insect Embryology in
898 Japan. H Ando, K Miya, editors. (ISEBU Co. Ltd.), p 203-213.
899
900 Kjer KM, Simon C, Yavorskaya M, Beutel RG. 2016. Progress, pitfalls and parallel
901 universes: a history of insect phylogenetics. J R Soc Interface 13:20160363.
902
903 Kobayashi Y, Ando H. 1990. Early embryonic development and external features of
904 developing embryos of the caddisfly, Nemotaulius admorsus (Trichoptera:
905 Limnephilidae). J Morphol 203:69-85.
906
907 Kobayashi Y, Suzuki H, Ohba N. 2003. Development of the pleuropodia in the
908 embryo of the glowworm Rhagophthalmus ohbai (Rhagophthalmidae, Coleoptera,
909 Insecta), with comments on their probable function. Proc Arthropod Embryol Soc
910 Jpn 38:19-26.

911

912 Konopova B, Zrzavy J. 2005. Ultrastructure, development, and homology of insect
913 embryonic cuticles. J Morphol 264:339-362.

914

915 Lambiase S, Grigolo A, Morbini P. 2003. Ontogenesis of pleuropodia in defferent
916 species of Blattaria (Insecta): a comparative study. Ital J Zool 70:205-212.

917

918 Langmead B, Trapnell C, Pop M, Salzberg SL. 2009. Ultrafast and memory-efficient
919 alignment of short DNA sequences to the human genome. Genome Biol 10:R25.

920

921 Larink O. 1983. Embryonic and postembryonic development of Machilidae and
922 Lepismatidae (Insecta: Archaeognatha). Entomol Gen 8:119-133.

923

924 Lemaitre B, Hoffmann J. 2007. The host defense of Drosophila melanogaster. Annu
925 Rev Immunol 25:697-743.

926

927 Lenaerts C, Van Wielendaele P, Peeters P, Vanden Broeck J, Marchal E. 2016.
928 Ecdysteroid signalling components in metamorphosis and development of the
929 desert locust, Schistocerca gregaria. Insect Biochem Mol Biol 75:10-23.

930

931 Lewis DL, DeCamillis M, Bennett RL. 2000. Distinct roles of the homeotic genes Ubx
932 and abd-A in beetle embryonic abdominal appendage development. Proc Natl Acad
933 Sci USA 97:4504-4509.

Li D, Zhang J, Wang Y, Liu X, Ma E, Sun Y, Li S, Zhu KY, Zhang J. 2015. Two chitinase 5 genes from Locusta migratoria: molecular characteristics and functional differentiation. Insect Biochem Mol Biol 58:46-54.

Liu HW, Wang LL, Tang X, Dong ZM, Guo PC, Zhao DC, Xia QY, Zhao P. 2018. Proteomic analysis of Bombyx mori molting fluid: Insights into the molting process. J Proteomics 173:115-125.

Locke M, Krishnan N. 1973. The formation of the ecdysial droplets and the ecdysial membrane in an insect. Tissue Cell 5:441-450.

Louvet JP. 1973. L'ultrastructure du pleuropode et son ontogenèse, chez l'embryon du phasme Carausius morosus Br. I. – Étude du pleuropode de l'embryon agé. Ann Sci Nat Zool 12:525-594.

Louvet JP. 1975. Premières observations sur l'ultrastructure du pleuropode chez le Criquet migrateur. C R Acad Sci Paris D 280: 1301-1304.

Louvet JP. 1983. Ultrastrucutre du pleuropode chez l'embryon du hanneton Rhizotrogus majalis Razoum (Coleoptera: Melolonthidae). Int J Insect Morphol Embryol 12:97-117.

957 Love MI, Huber W, Anders S. 2014. Moderated estimation of fold change and
958 dispersion for RNA-seq data with DESeq2. Genome Biol 15:550.
959
960 Machida R. 1981. External features of embryonic development of a jumping
961 bristletail, Pedetontus unimaculatus Machida (Insecta, Thysanura, Machilidae). J
962 Morphol 168:339-355.
963
964 Machida R, Tojo K, Tsutsumi T, Uchifune T, Klass K-D, Picker MD, Pretorius L. 2004.
965 Embryonic development of heel-walkers: reference to some prerevolutionary stages
966 (Insecta: Mantophasmatodea). Proc Arthropod Embryol Soc Jpn 39:31-39.
967
968 Marchal E, Badisco L, Verlinden H, Vandersmissen T, Van Soest S, Van Wielendaele P,
969 Vanden Broeck J. 2011. Role of the Halloween genes, Spook and Phantom in
970 ecdysteroidogenesis in the desert locust, Schistocerca gregaria. J Insect Physiol
971 57:1240-1248.
972
973 Marchal E, Verlinden H, Badisco L, Van Wielendaele P, Vanden Broeck J. 2012. RNAi-
974 mediated knockdown of Shade negatively affects ecdysone-20-hydroxylation in the
975 desert locust, Schistocerca gregaria. J Insect Physiol 58:890-896.
976
977 Mashimo Y, Beutel RG, Dallai R, Lee CY, Machida R. 2013. Embryonic development of
978 Zoraptera with special reference to external morphology, and its phylogenetic
979 implications (Insecta). J Morphol 275:295-312.

Miller A. 1940. Embryonic membranes, yolk cells, and morphogenesis of the stonefly Pteronarcys proteus Newman (Plecoptera: Pteronarcidae). Ann Entomol Soc Amer 33:437-477.

Mohamed AA, Zhang L, Dorrah MA, Elmogy M, Yousef HA, Bassal TT, Duvic B. 2016. Molecular characterization of a c-type lysozyme from the desert locust, Schistocerca gregaria (Orthoptera: Acrididae). Dev Comp Immunol 61:60-69.

Mortazavi A, Williams BA, McCue K, Schaeffer L, Wold B. 2008. Mapping and quantifying mammalian transcriptomes by RNA-Seq. Nat Methods **5**:621–628.

Miyakawa K. 1979. Embryology of the dobsonfly, Protohermes grandis Thunberg (Megaloptera: Corydalidae), I. Changes in External form of the embryo during development. Kontyû 47: 367-375.

Nijhout HF. 1994. Insect hormones. Princeton: Princeton University Press.

Niwa R, Matsuda T, Yoshiyama T, Namiki T, Mita K, Fujimoto Y, Kataoka H. 2004. CYP306A1, a cytochrome P450 enzyme, is essential for ecdysteroid biosynthesis in the prothoracic glands of Bombyx and Drosophila. J Biol Chem 279:35942-35949.

1002 Niwa R, Niwa YS. 2014. Enzymes for ecdysteroid biosynthesis: their biological
1003 functions in insects and beyond. Biosci Biotechnol Biochem 78:1283-1292.
1004
1005 Noh MY, Muthukrishnan S, Kramer KJ, Arakane Y. 2018. A chitinase with two
1006 catalytic domains is required for organization of the cuticular extracellular matrix
1007 of a beetle. PLoS Genet 14:e1007307.
1008
1009 Norling U. 1982. Structure and ontogeny of the lateral abdominal gills and the
1010 caudal gills in Euphaenidae (Odonata: Zygoptera) larvae. Zool Jb Anat 107:343-389.
1011
1012 Novak VJA, Zambre SK. 1974. To the problem of structure and function of
1013 pleuropodia in Schistocerca gregaria FORSKÅL embryos. Zool Jb Physiol 78:344-
1014 355.
1015
1016 Ou Q, Zeng J, Yamanaka N, Brakken-Thal C, O'Connor MB, King-Jones K. 2016. The
1017 Insect Prothoracic Gland as a Model for Steroid Hormone Biosynthesis and
1018 Regulation. Cell Rep 16:247-262.
1019
1020 Pagès H, Aboyoun P, Gentleman R and DebRoy S. 2017. Biostrings: Efficient
1021 manipulation of biological strings. R package version 2.46.0.
1022
1023 Panfilio KA. 2008. Extraembryonic development in insects and the acrobatics of
1024 blastokinesis. Dev Biol 313:471-491.

Pertea G, Huang X, Liang F, Antonescu V, Sultana R, Karamycheva S, Lee Y, White J, Cheung F, Parvizi B, Tsai J, Quackenbush J. 2003. TIGR Gene Indices clustering tools (TGICL): a software system for fast clustering of large EST datasets. Bioinformatics 19:651-652.

Petryk A, Warren JT, Marqués G, Jarcho MP, Gilbert LI, Kahler J, Parvy JP, Li Y, Dauphin-Villemant C, O'Connor MB. 2003. Shade is the Drosophila P450 enzyme that mediates the hydroxylation of ecdysone to the steroid insect molting hormone 20-hydroxyecdysone. Proc Natl Acad Sci USA 100:13773-13778.

Pesch YY, Riedel D, Patil KR, Loch G, Behr M. 2016. Chitinases and Imaginal disc growth factors organize the extracellular matrix formation at barrier tissues in insects. Sci Rep 6:18340.

Prpic NM, Wigand B, Damen WG, Klingler M. 2001. Expression of dachshund in wild-type and Distal-less mutant Tribolium corroborates serial homologies in insect appendages. Dev Genes Evol 211:467-477.

Qu M, Ma L, Chen P, Yang Q. 2014. Proteomic analysis of insect molting fluid with a focus on enzymes involved in chitin degradation. J Proteome Res 13:2931-2940.

1047 R Development Core Team. 2008. R: A language and environment for statistical
1048 computing. R Foundation for Statistical Computing, Vienna, Austria. ISBN 3-900051-
1049 07-0.
1050
1051 Rau A, Gallopin M, Celeux G, Jaffrezic F. 2013. Data-based filtering for replicated
1052 high-throughput transcriptome sequencing experiments. Bioinformatics 29:2146-
1053 2152.
1054
1055 Rathke H. 1844. Zur Entwickelungsgeschichte der Maulwurfsgrille (Gryllotalpa
1056 vulgaris). Arch Anat Physiol wiss Med 27-37.
1057
1058 Reynolds SE, Samuels R. 1996. Physiology and biochemistry of insect moulting fluid.
1059 Adv In Insect Phys 26:157-232.
1060
1061 Rong S, Li DQ, Zhang XY, Li S, Zhu KY, Guo YP, Ma EB, Zhang JZ. 2013. RNA
1062 interference to reveal roles of β-N-acetylglucosaminidase gene during molting
1063 process in Locusta migratoria. Insect Sci 20:109-119.
1064
1065 Roonwall ML. 1937. Studies on the embryology of the African migratory locust,
1066 Locusta migratoria migratorioides Reiche and Frm. (Orthoptera, Acrididae). II.
1067 Organogeny. Philos Trans R Soc Lond B Biol Sci 227: 175-244.
1068

1069 Rost MM, Poprawa I, Klag J. 2004. Ultrastructure of the pleuropodium in 8-d-old
1070 embryos of Thermobia domestica (Packard) (Insecta, Zygentoma). Ann Entomol Soc
1071 Amer 97:541-547.
1072
1073 Schulz MH, Zerbino DR, Vingron M, Birney E. 2012. Oases: robust de novo RNA-seq
1074 assembly across the dynamic range of expression levels. Bioinformatics 28:1086-
1075 1092.
1076
1077 Shi L, Paskewitz SM. 2004. Identification and molecular characterization of two
1078 immune- responsive chitinase-like proteins from Anopheles gambiae. Insect Mol
1079 Biol 13:387–398.
1080
1081 Shutts JH. 1952. Some characteristics of the hatching enzyme in the eggs of
1082 Melanoplus differentialis (Thomas). Proc S Dak Acad Sci 31:158-163.
1083
1084 Simão FA, Waterhouse RM, Ioannidis P, Kriventseva EV, Zdobnov EM. 2015. BUSCO:
1085 assessing genome assembly and annotation completeness with single-copy
1086 orthologs. Bioinformatics. 31:3210-3212.
1087
1088 Slifer EH. 1937. The origin and fate of the membranes surrounding the grasshopper
1089 egg; together with some experiments on the source of the hatching enzyme. Q J Micr
1090 Sci 79:493-506.
1091

1092 Slifer EH. 1938. A cytological study of the pleuropodia of Melanoplus differentialis
1093 (Orthoptera, Acrididae) which furnishes new evidence that they produce the
1094 hatching enzyme. J Morphol 63:181-206.
1095
1096 Stanley MSM, Grundmann AW. 1970. The embryonic development of Tribolium
1097 confusum. Ann Entomol Soc Amer 63:1248-1256.
1098
1099 Stay B. 1977. Fine structure of two types of pleuropodia in Diploptera punctata
1100 (Dictyoptera: Blaberiadae) with observations on their permeability. Int J Insect
1101 Morphol Embryol 6:67-95.
1102
1103 Sugahara R, Tanaka S and Shiotsuki T. 2017. RNAi-mediated knockdown of SPOOK
1104 reduces ecdysteroid titers and causes precocious metamorphosis in the desert
1105 locust Schistocerca gregaria. Dev Biol 429:71-80.
1106
1107 Sui Y-P, Liu X-B, Chai L-Q, Wang J-X, Zhao X-F. 2009. Characterization and influences
1108 of classical insect hormones on the expression profiles of a molting
1109 carboxypeptidase A from the cotton bollworm (Helicoverpa armigera). Insect Mol
1110 Biol 18:353-363.
1111
1112 Supek F, Bošnjak M, Škunca N, Šmuc T. 2011. REVIGO Summarizes and Visualizes
1113 Long Lists of Gene Ontology Terms. PLoS ONE 6: e21800.
1114

1115 Tanaka M, Kobayashi Y, Ando H. 1985. Embryonic development of the nervous
1116 system and other ectodermal derivatives in the primitive moth, Endoclita sinensis
1117 (Lepidoptera, Hepialidae). In: Ando H, Miya K, editors. Recent Advances in Insect
1118 Embryology in Japan. Tsukuba: Isebu Co. Ltd. p 215-229.
1119
1120 Tanizawa T, Ando H, Tojo K. 2007. Notes on the pleuropodia in the giant water bug
1121 Appasus japonicus (Heteroptera, Belostomatidae). Proc Arthropod Embryol Soc Jpn
1122 42:9-11.
1123
1124 Tarazona S, García-Alcalde F, Dopazo J, Ferrer A, Conesa A. 2011. Differential
1125 expression in RNA-seq: a matter of depth. Genome Res 21:2213-2223.
1126
1127 Tear G, Akam M, Martinez-Arias A. 1990. Isolation of an abdominal-A gene from the
1128 locust Schistocerca gregaria and its expression during early embryogenesis.
1129 Development 110:915-925.
1130
1131 Tsutsumi K, Machida R. 2006. Embryonic development of a snakefly, Inocellia
1132 japonica Okamoto: an outline (Insecta: Neuroptera, Raphidiodea). Proc Arthropod
1133 Embryol Soc Jpn 41: 37-45.
1134
1135 Uchifune T, Machida R. 2005. Embryonic development of Galloisiana yuasai Asahina,
1136 with special reference to external morphology (insecta: Grylloblattodea). J Morphol
1137 266:182-207.

1138

1139 Untergasser A, Nijveen H, Rao X, Bisseling T, Geurts R, and Leunissen JMA. 2007.
1140 Primer3Plus, an enhanced web interface to Primer3. Nucleic Acids Research 35:
1141 W71-W74.

1142

1143 Viscuso R, Sottile L. 2008. Fine structure of pleuropodia in three species of Insecta
1144 Orthoptera during embryonic development. Ital J Zool (Modena) 75: 11-19.

1145

1146 Xi Y, Pan PL, Ye YX, Yu B, Xu HJ, Zhang CX. 2015. Chitinase-like gene family in the
1147 brown planthopper, Nilaparvata lugens. Insect Mol Biol 24:29-40.

1148

1149 Warren JT, Petryk A, Marques G, Jarcho M, Parvy JP, Dauphin-Villemant C, O'Connor
1150 MB, Gilbert LI. 2002. Molecular and biochemical characterization of two P450
1151 enzymes in the ecdysteroidogenic pathway of Drosophila melanogaster. Proc Natl
1152 Acad Sci USA 99:11043-11048.

1153

1154 Warren JT, Petryk A, Marqués G, Parvy JP, Shinoda T, Itoyama K, Kobayashi J, Jarcho
1155 M, Li Y, O'Connor MB, Dauphin-Villemant C, Gilbert LI. 2004. Phantom encodes the
1156 25-hydroxylase of Drosophila melanogaster and Bombyx mori: a P450 enzyme
1157 critical in ecdysone biosynthesis. Insect Biochem Mol Biol 34:991-1010.

1158

1159 Waterhouse RM, Seppey M, Simão FA, Manni M, Ioannidis P, Klioutchnikov G,
1160 Kriventseva EV, Zdobnov EM. 2018. BUSCO applications from quality assessments to
1161 gene prediction and phylogenomics. Mol Biol Evol 35:543-548.
1162
1163 Wei Z, Yin Y, Zhang B, Wang Z, Peng G, Cao Y, Xia Y. 2007. Cloning of a novel protease
1164 required for the molting of Locusta migratoria manilensis. Dev Growth Differ
1165 49:611-621.
1166
1167 Wheeler WMM. 1889. On the appendages of the first abdominal segment of embryo
1168 insects. Trans Wis Acad Sci Arts Lett 8:87-140, pls 1-3.
1169
1170 Yan J, Cheng Q, Narashimhan S, Li CB, Aksoy S. 2002. Cloning and functional
1171 expression of a fat body-specific chitinase cDNA from the tsetse fly, Glossina
1172 morsitans morsitans. Insect Biochem Mol Biol 32:979–989.
1173
1174 Young MD, Wakefield MJ, Smyth GK and Oshlack A. 2010. Gene ontology analysis for
1175 RNA-seq: accounting for selection bias. Genome Biol 11:R14.
1176
1177 Zerbino DR, Birney E. 2008. Velvet: algorithms for de novo short read assembly
1178 using de Bruijn graphs. Genome Res 18:821-829.
1179

1180 Zhang J, Lu A, Kong L, Zhang Q, Ling E. 2014. Functional analysis of insect molting
1181 fluid proteins on the protection and regulation of ecdysis. J Biol Chem 289:35891-
1182 35906.
1183
1184 Zhang H, Shinmyo Y, Mito T, Miyawaki K, Sarashina I, Ohuchi H, Noji S. 2005.
1185 Expression patterns of the homeotic genes Scr, Antp, Ubx, and abd-A during
1186 embryogenesis of the cricket Gryllus bimaculatus. Gene Expr Patterns 5:491-502.
1187
1188 Zhu Q, Arakane Y, Beeman RW, Kramer, KJ, Muthukrishnan S. 2008. Functional
1189 specialization among insect chitinase family genes revealed by RNA interference.
1190 Proc Natl Acad Sci USA 105:6650-6655.
1191
1192 Zhu KY, Merzendorfer H, Zhang W, Zhang J, Muthukrishnan S. 2016. Biosynthesis,
1193 Turnover, and Functions of Chitin in Insects. Annu Rev Entomol 61:177-196.

1194 **FIGURE 1**

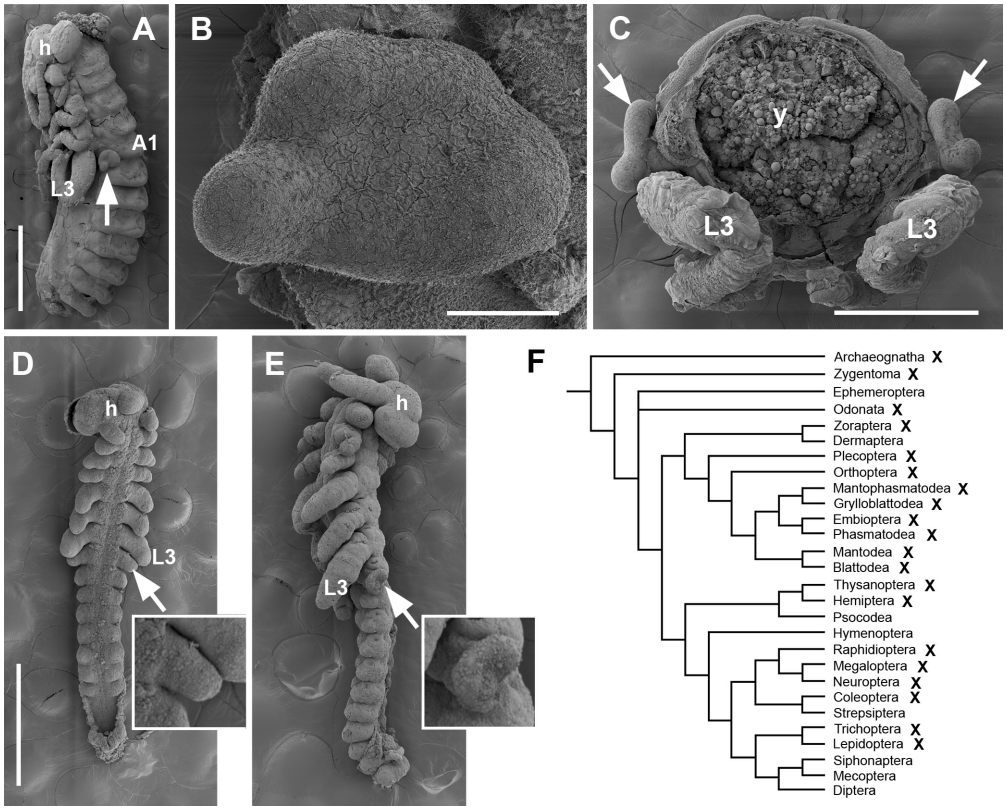

1195

1196 **Figure 1. Pleuropodia are limb-derived organs on A1 of insect embryos.** (A)-

1197 (C): External morphology of fully developed pleuropodia of *Schistocerca gregaria*.

1198 (A) Embryo before dorsal closure (yolk was removed). (B) Enlarged left

1199 pleuropodium. (C) Cross section through A1. (D) and (E): Pleuropodia originate by a

1200 modification of a limb bud. (D) Early embryo: all appendages are similarly looking

1201 buds. (E) Older embryo: future legs elongate and the buds on A1 start to take shape

1202 of pleuropodia. (F) Insect phylogenetic tree showing the presence of pleuropodia

1203 among “orders”. The cross marks “orders” where at least some species develop

1204 pleuropodia. Phylogeny from Kjer et al., 2016, other references in the text. (A)-(E)

1205 are scanning electron microscopy (SEM) micrographs. Pleuropodium is marked with

an arrow. A1, the first abdominal segment; h, head; L3, hind (third) leg; y, yolk. Scale bars: in (A), 1 mm; in (B), 100 μm; in (C); 500 μm; in (D), for (D) and (E), 500 μm.

1208 **FIGURE 2**

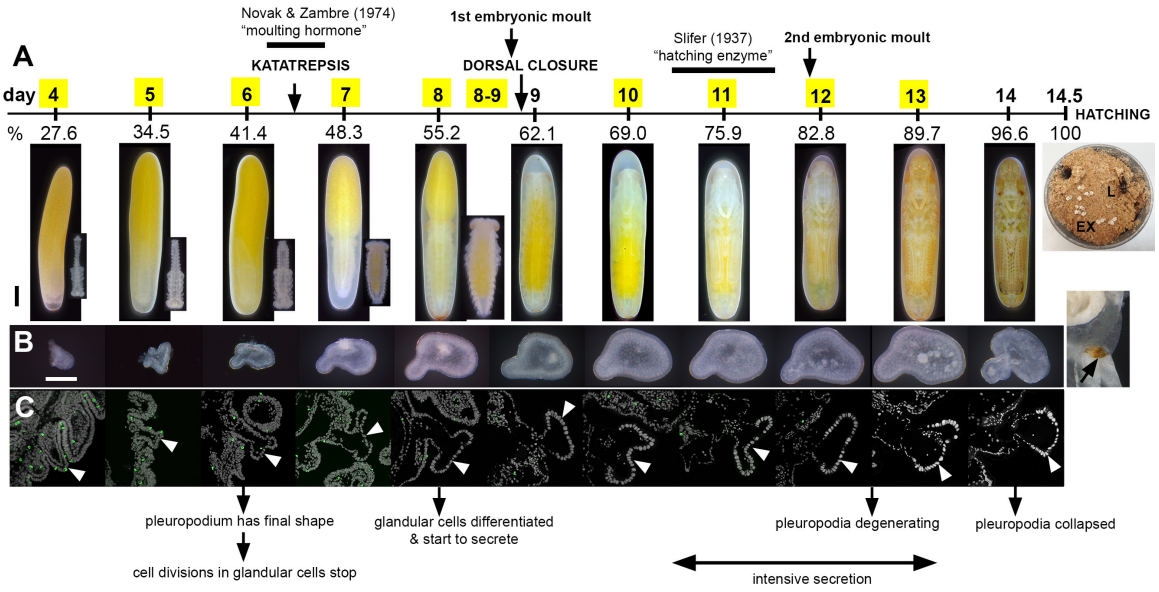

1209

1210 **Figure 2. Summary of the development of pleuropodia in *Schistocerca***

1211 **embryos.** (A) Scheme of *Schistocerca* embryogenesis marking key developmental

1212 events in the embryos and timing of the two experiments on pleuropodia. Numbers

1213 above the scale are days from egg-laying, numbers below the scale are percent of

1214 embryonic developmental time. Yellow boxes indicate the stages that were sampled

1215 for RNA-seq. Eggs with the developing embryos at each stage are shown below the

1216 scale, insets for the 4-8 day stages show the embryo dissected out from the egg. (B)

1217 External features of the developing pleuropodia; after hatching part of the stretched

1218 exuvia is shown; the degenerated pleuropodium is marked with an arrow. (C)

1219 Paraffin sections through the pleuropodium and surrounding tissue. Pleuropodia

1220 are marked with arrowheads. PH3 (green) detects cell divisions in the immature

1221 glandular cells (tip of appendage bud) on day 4 and 5, not in later stages. The

1222 pleuropodial stalk cells, haemocytes entering the pleuropodia and cells in other

1223 tissues were labeled. Nuclei (grey) enlarge from day 6. The text below the pictures
1224 refers to the main events in the glandular cells. EX, exuvia; L, larva. Scale bars: in (A)
1225 (eggs), 1 mm; in (B), 0.2 mm. Background was cleaned in photos in A (see Materials
1226 and Methods).

1227 **FIGURE 3**

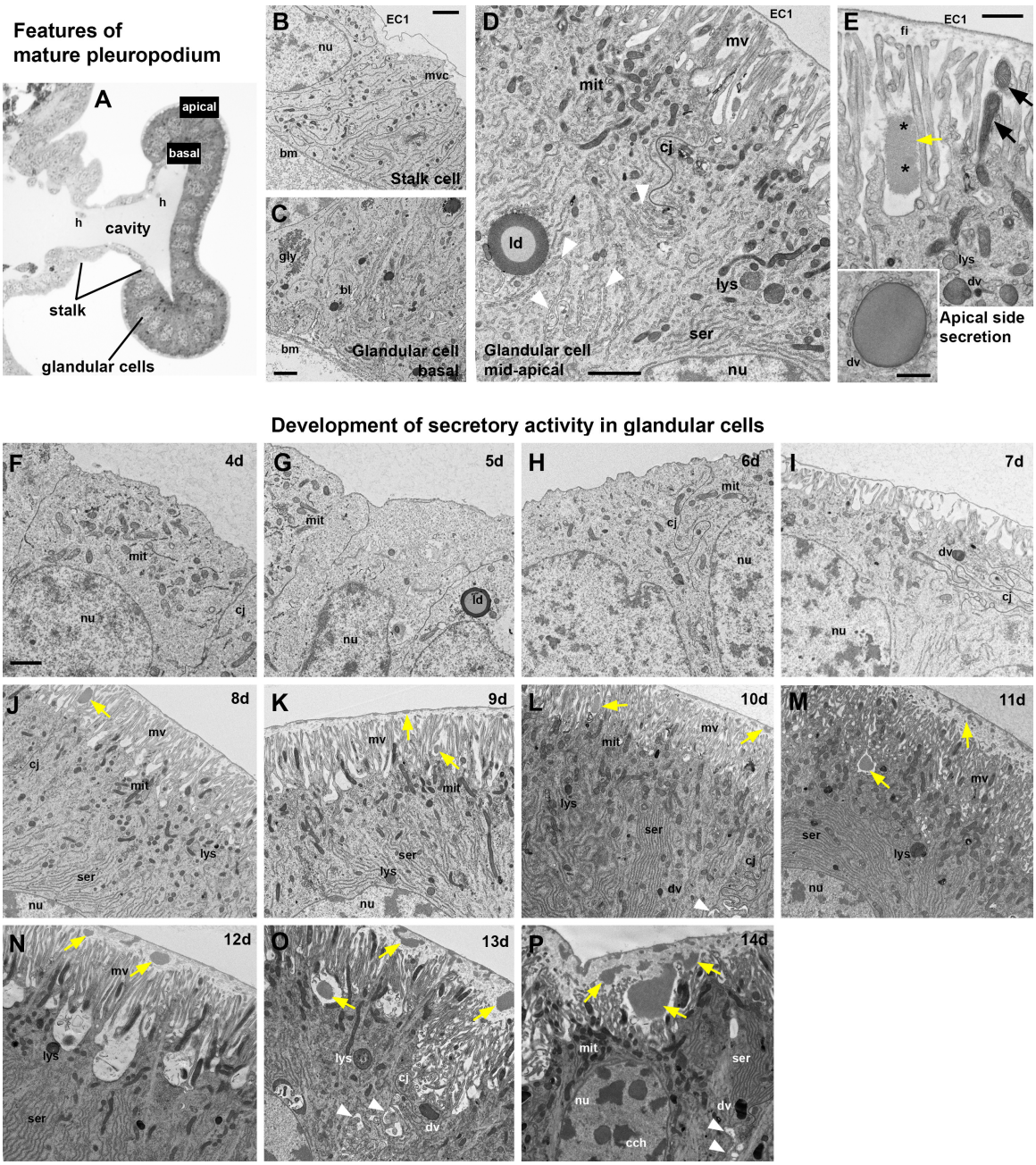

1228

1229 **Figure 3. Ultrastructure of the *Schistocerca* pleuropodia.** (A)-(E) Main features

1230 of the cells in the fully formed pleuropodia. Pleuropodia just before dorsal closure

1231 are shown. (A) Cross section through the pleuropodium. (B) Stalk cell. The short

1232 microvilli at the apical side are associated with the deposition of fibres in the

1233 embryonic cuticle ("the first embryonic cuticle", EC1). (C)-(E) Glandular cells. In (D)
1234 the white arrowheads mark the spaces between neighboring cells. In (E) the black
1235 arrows mark mitochondria inside the microvilli and the asterisks mark spots of
1236 different electron-density in the secreted granule. Note that the secretion granule is
1237 located at the base of the microvilli (brush-border); the tips of the microvilli
1238 produce fibrous material that is a part of the embryonic cuticle EC1. (F)-(P)
1239 Ontogenesis of the glandular cells. Note the development of the microvilli (brush
1240 border) and the onset of secretion (appearance of secretion granules within and
1241 above the microvilli). On day 8 (J) the glandular cells are differentiated, on day 12
1242 (N) patches of the apical side elevate, on day 13 (O) the organelles are disorganized,
1243 on day 14 (P) cytoplasm is electron dense (cells shrink), chromatin condensed, but
1244 large secretion granules are still present at the base of microvilli and above them.
1245 (A) is a toluidine blue stained semithin section, (B)-(P) TEM micrographs. Secretion
1246 granules are marked with yellow arrows. bm, basement membrane; bl, basal
1247 labyrinth (infolding of the basal plasma membrane); cj, cell junction; dv, dense
1248 vesicle; EC1, the first embryonic cuticle; gly, glycogene; ld, lipid droplet; mit,
1249 mitochondria; mv, microvilli; nu, nucleus; ser, smooth endoplasmic reticulum. Scale
1250 bars: in (B), (C), (D), (E) and (F) for (F)-(P), 2 μm; inset in (E), 500 nm.

FIGURE 4

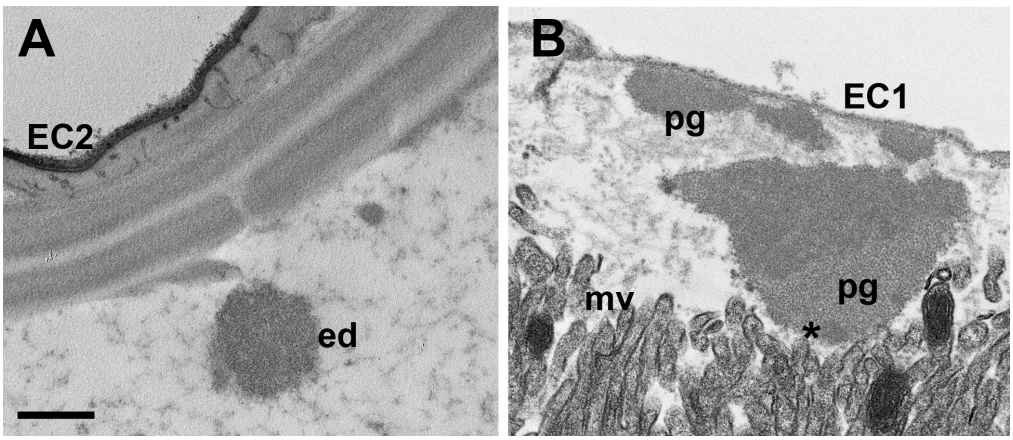

Figure 4. Granules secreted from the pleuropodia resemble ecdysial droplets.

(A) Ecdysial droplet secreted during the second embryonic moult by hind leg epidermis. (B) Granules secreted from pleuropodia at the same developmental stage. The pleuropodial granules are typically larger, less compact and with non-homogeneous electrondensity. The "spot" of a different electron-density in the pleuropodial granules is marked with an asterisk. EC1, EC2, the first and second embryonic cuticles; ed, ecdysial droplets; mv, microvilli; pg, granules secreted from the pleuropodia. Scale bar: for (A) and (B), 500 nm.

1261 **FIGURE 5**

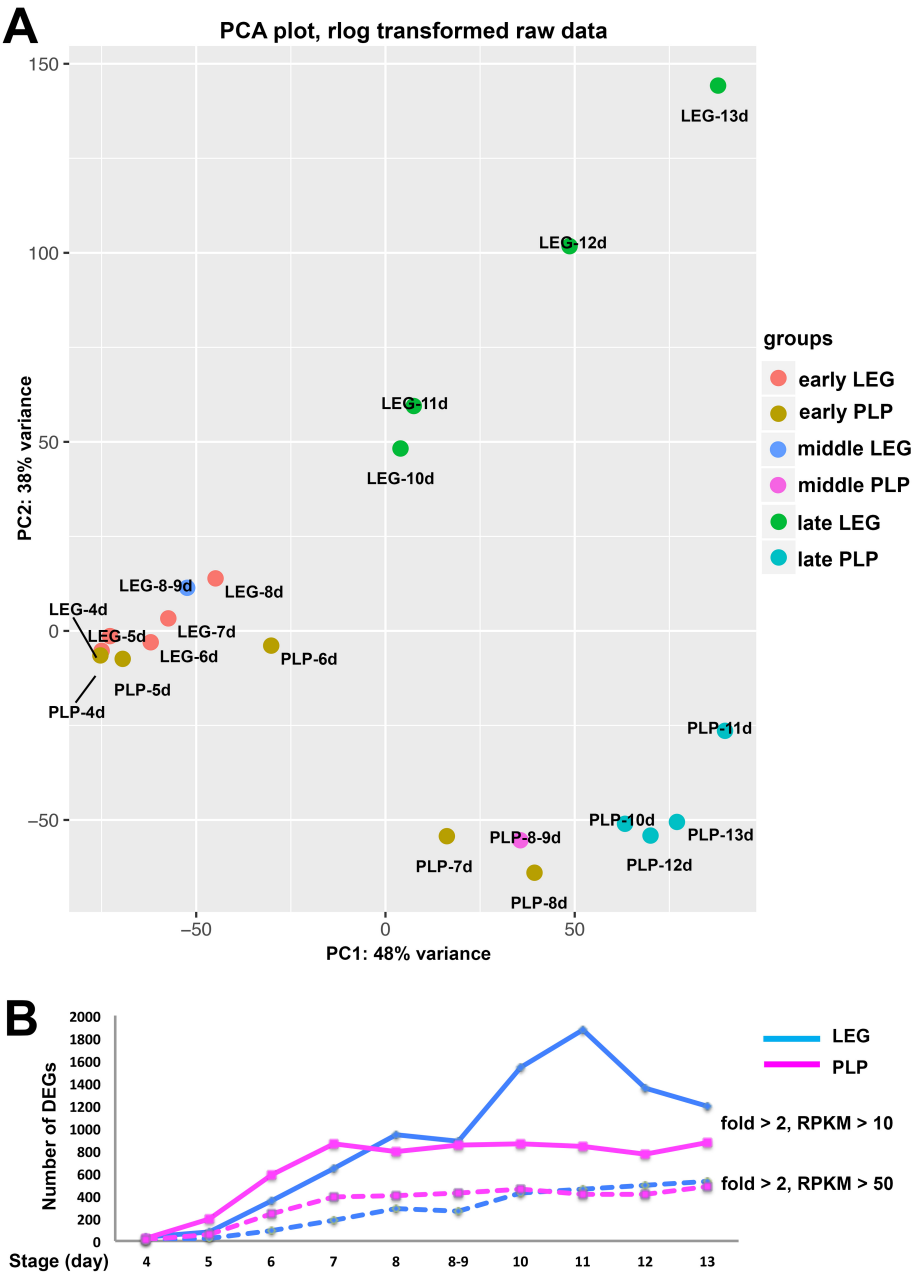

1262

1263 **Figure 5. Legs and pleuropodia become genetically more different as**

1264 **development progresses.** (A) PCA on genes expressed in legs and pleuropodia at

1265 ten embryonic stages (rlog transformed read counts). Samples from young embryos

1266 are genetically more similar and cluster together, while samples from advanced

1267 stages are genetically more distant and also separated on the plot. (B) Number of
1268 DEGs at two levels of stringency (RPKM > 10 and fold change > 2 was considered as
1269 a threshold for a gene to be differentially expressed). LEG, DEGs downregulated in
1270 pleuropodia and upregulated in legs, PLP, DEGs upregulated in pleuropodia and
1271 downregulated in legs.

1272 **FIGURE 6**

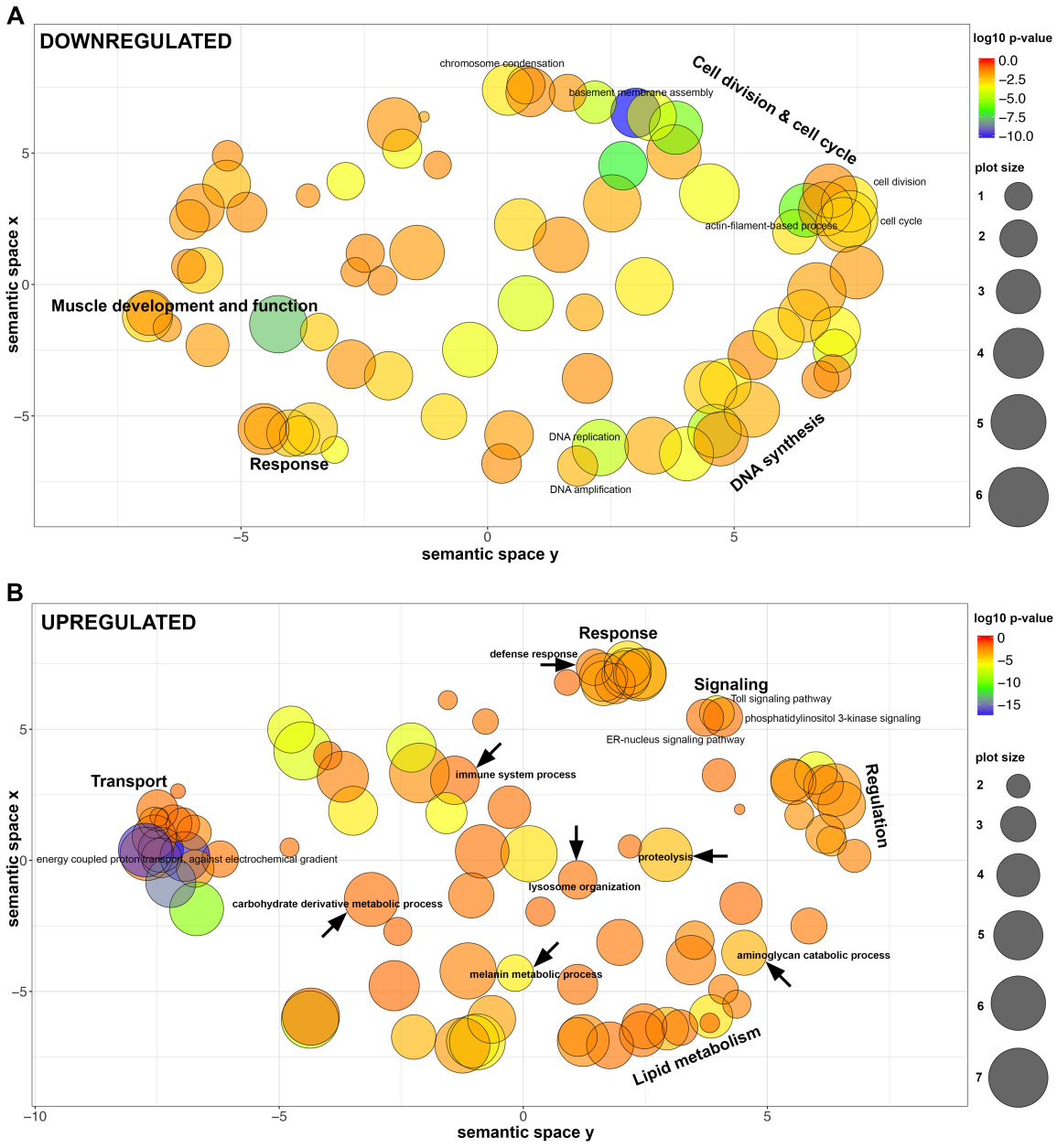

1273

1274 **Figure 6. Dot plot visualization of GO terms enriched in DEGs in the highly**

1275 **secreting pleuropodia.** Representative groups of GO terms enriched in genes that

1276 are (A) downregulated in pleuropodia (in comparison to legs) and (B) upregulated

1277 in pleuropodia. Major clusters are labeled. Relevant GOs are marked with an arrow.

1278 Bubble color indicates the p-value of the GO term, the size indicates the frequency of

1279 the GO term in the underlying Gene Ontology Annotation (GOA) database (bubbles

1280 of more general terms are larger).

FIGURE 7

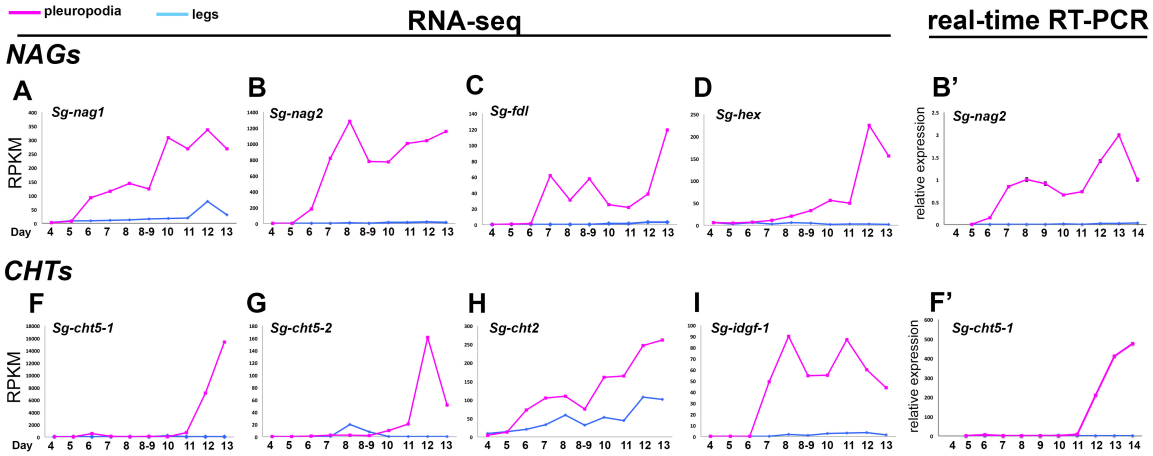

Figure 7. Expression profiles of NAGs and CHTs upregulated in the pleuropodia of *Schistocerca* across development. Top row: NAGs, bottom row: CHTs. (A-D) and (F)-(I): RNA-seq, Expression in single-sample sequencing is shown. (B') and (F'): real-time RT-PCR. (B') is the same gene as in (B) and (F') is the same gene as in (F). Analysis of 3-4 technical replicates is shown. Expression in day 8 was set as 1.

1289 **FIGURE 8**

1290

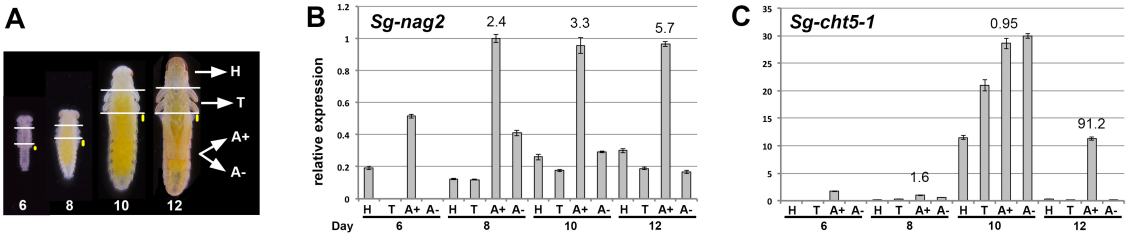

1291 **Figure 8. Real-time RT-PCR expression analysis of *Sg-nag2* and *Sg-cht5-1* on**

1292 **cDNA from parts of *Schistocerca* embryos.** (A) cDNA was prepared from mRNAs

1293 isolated from parts of embryos at the age of 6, 8, 10 and 12 days: H, head; T, thorax;

1294 A+, abdomen with pleuropodia; A-, abdomen without pleuropodia. For each age the

1295 same number of body parts was used (5-10) and RNA was resuspended in the same

1296 volume of water. The size of the pleuropodium is indicated by the yellow dot. (B)

1297 and (C): expression of *Sg-nag2* and *Sg-cht5-1*, respectively. Analysis of 3-4 technical

1298 replicates is shown. Expression in A+8 (abdomen with pleuropodia at stage when

1299 the organs first become differentiated) was set as 1. Numbers above A+ expression

1300 is fold change from A- of the same age.

1301 **FIGURE 9**

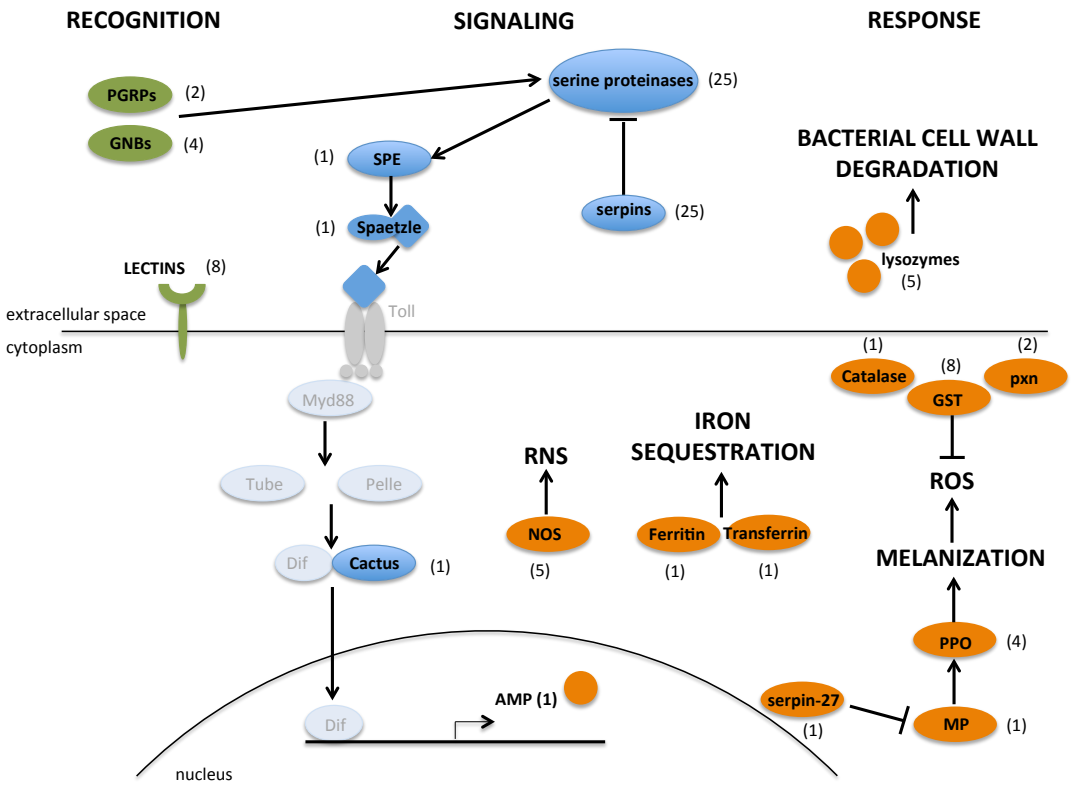

1302

1303 **Figure 9. Schematic representation of key immunity-related genes expressed**

1304 **in the highly secreting pleuropodia of *Schistocerca*.** Proteins whose transcripts

1305 were found in the pleuropodia are in black, number in the brackets is the number of

1306 upregulated transcripts. Proteins whose transcripts were not upregulated are in

1307 grey. Out of the total 25 serine proteases and 25 serpins, 14 and 15 are known to

1308 function in Toll signaling, respectively. AMP, antimicrobial peptide; GNBP, gram-

1309 negative bacteria-binding protein; GST, glutathione S-transferase; MP, melanization

1310 protease; NOS, nitric oxide synthase; PGRP, peptidoglycan recognition protein; PPO,

1311 pro-phenoloxidase; pxn, peroxiredoxin; RNS, reactive nitrogen species; ROS,

1312 reactive oxygen species; SPE, Spaetzle-processing enzyme.

1313 **FIGURE 10**

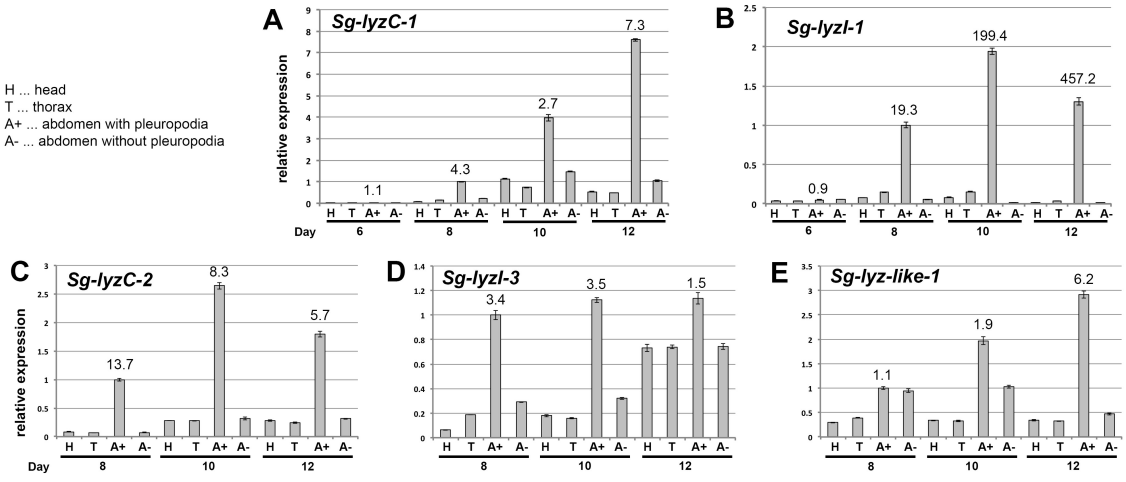

1314

1315 **Figure 10. Real-time RT-PCR expression analysis of genes for lysozymes on**

1316 **cDNA from parts of *Schistocerca* embryos.** cDNA was prepared from mRNAs

1317 isolated from parts of embryos at the age of 6, 8, 10 and 12 days. For each age the

1318 same number of body parts was used (5-10) and RNA was resuspended in the same

1319 volume of water. Analysis of 3-4 technical replicates is shown. Expression in A+8

1320 (abdomen with pleuropodia at stage when the organs first become differentiated)

1321 was set as 1. Numbers above A+ expression is fold change from A- of the same age.

1322 **Table 1. Top ten percent of the most abundant transcripts upregulated in the**

1323 **highly secreting pleuropodia of *Schistocerca*.**

1324

Transcript ID	Protein	Characteristics	Immunity[a]	Cuticle digestion[b]	RPKM		Fold change
					legs	pleuropodia	
SgreTa0017702	x				23.07	15186.05	658.36
SgreTa0007897	C-type lysozyme	anti-bacterial protein	x		42.93	14452.15	336.64
SgreTa0002988	Uncharacterized, contains DUF4773 domain				15.16	9112.05	601.19
SgreTa0005052	x				13.37	7950.98	594.48
SgreTa0001636	Serine protease	proteolysis	x	x	49.38	7578.31	153.48
SgreTa0008851	Chitin binding Peritrophin-A	perotrophic matrix protein			9.12	6836.42	749.88
SgreTa0017707	I-type lysozyme	anti-bacterial protein	x		12.20	6712.31	550.26
SgreTa0007042	x				7.04	6650.18	944.25
SgreTa0004599	Alpha-tocopherol transfer protein	intermembrane lipid transfer			8.99	5848.12	650.71
SgreTa0009217	x				5.03	5384.56	1070.14
SgreTa0003175	Collagen				32.25	5220.96	161.87
SgreTa0007886	Alpha-N-acetylgalactosaminidase	carbohydrate catabolism			3.85	4372.63	1134.69
SgreTa0002109	x				2.20	3016.31	1372.07
SgreTa0017715	Serine protease, Snake-like	proteolysis, Toll signaling	x	x	70.55	2947.46	41.78
SgreTa0017664	Chitinase 5	cuticular chitin degradation		x	79.32	2620.11	33.03
SgreTa0002467	Neutral endopeptidase 24.11	proteolysis		x	62.26	2282.01	36.66
SgreTa0004397	x				11.21	2266.30	202.21
SgreTa0002828	x				1.77	2188.14	1234.00
SgreTa0006539	Serpin, 88E-like	serine protease inhibitor	x		32.42	2152.14	66.38
SgreTa0001321	Glycosyl hydrolase, Myrosinase 1-like	carbohydrate catabolism			3.93	2070.40	527.16
SgreTb0011177	x				1.38	1884.79	1369.32
SgreTa0008335	x				54.24	1812.38	33.41
SgreTa0003635	Alpha-tocopherol transfer protein	intermembrane lipid transfer			2.23	1800.68	806.99
SgreTb0003860	Serine protease, H2-like	proteolysis	x	x	77.42	1727.41	22.31
SgreTa0013418	x				0.87	1484.98	1710.66
SgreTa0014009	Angiotensin-converting enzyme	proteolysis		x	65.76	1457.47	22.16
SgreTa0006966	Pro-phenol oxidase subunit 2	immunity, melanization	x		144.78	1347.43	9.31
SgreTa0000425	6-phosphofructo-2-kinase	glycolysis			93.52	1346.50	14.40
SgreTa0003661	Serine protease, Easter-like	proteolysis	x	x	29.50	1332.79	45.18
SgreTa0006960	Glutamate dehydrogenase mitochondrial	nitrogen and glutamate metabolism			172.56	1327.45	7.69
SgreTa0017670	Xaa-Pro aminopeptidase	proteolysis		x	2.89	1322.01	457.96
SgreTb0000759	Cathepsin L	proteolysis, lysosomal enzyme		x	105.63	1308.36	12.39
SgreTa0014684	x				1.30	1294.87	994.80
SgreTa0007025	Insect pheromone-binding protein A10/OS-D	chemoreception			1.77	1224.20	692.95
SgreTa0006282	Cytochrome P450 CYP4G102	synthesis of hydrocarbons, anti-dehydration			2.91	1196.27	410.93
SgreTa0009515	Sensory neuron membrane protein, 1-like	chemoreception			3.33	1188.81	357.50
SgreTa0008528	C-type lysozyme	anti-bacterial protein	x		8.61	1159.55	134.71
SgreTa0009095	Catalase	redox homeostasis	x		355.15	1158.27	3.26
SgreTb0039135	x				3.53	1119.22	316.71
SgreTa0001486	Lipopolysaccharide-induced tumor necrosis factor-alpha factor homolog	lysosomal degradation			45.83	1109.33	24.20
SgreTb0039012	x				14.29	1060.82	74.25
SgreTa0009747	Serpin (27-like)	serine protease inhibitor, melanization	x		14.49	1054.67	72.80
SgreTa0013400	Peroxiredoxin, 5-llke	redox homeostasis	x		101.10	1034.15	10.23
SgreTa0017395	x				5.08	1004.86	197.64
SgreTa0017712	x				15.59	990.41	63.53
SgreTa0005600	Beta-N-acetylglucosaminidase NAG2	cuticular chitin degradation		x	15.10	939.60	62.21
SgreTa0000783	Serine protease, Snake-like	proteolysis	x	x	4.30	917.47	213.59
SgreTa0006651	Uncharacterized, contains Transcription activator MBF2 domain				1.62	907.98	561.49
SgreTa0017657	Putative serine protease, K12H4.7-like / Serine carboxypeptidase	proteolysis		x	2.31	904.26	391.60
SgreTa0017700	Peroxidase	redox homeostasis	x		5.36	874.51	163.25
SgreTa0002600	Uncharacterized, contains DUF3421 domain				0.97	870.73	894.35
SgreTb0019827	Tob	antiproliferative protein,			141.26	846.86	5.99

		transcription corepressor					
SgreTa0017854	x				0.85	838.89	981.74
SgreTa0007774	Lysosomal-associated membrane protein	lysosomal membrane protein			185.20	822.81	4.44
SgreTa0015156	x				27.45	804.82	29.32
SgreTa0007809	Tetraspanin	scaffolding protein in cell membrane			63.04	799.76	12.69
SgreTa0004471	Leucine rich repeat	membrane glycoprotein			74.88	797.35	10.65
SgreTa0004278	Fatty acyl-CoA reductase, waterproof-like	lipid metabolism			1.75	733.39	417.99
SgreTa0014626	V-type proton ATPase proteolipid subunit	proton transporting ATPase			190.76	708.56	3.71
SgreTa0016256	Bax inhibitor 1	negative regulation of apoptosis and autophagy			237.58	692.52	2.91
SgreTa0001469	Sodium/potassium-transporting ATPase subunit alpha	sodium:potassium exchanging ATPase			119.60	685.51	5.73
SgreTa0007426	Serine protease, Easter-like	proteolysis	x	x	0.66	673.43	1023.60
SgreTa0007081	Vigilin	RNA binding, sterol metabolism			247.46	655.61	2.65
SgreTa0013328	Ferritin	iron ion transport, iron sequestration	x		238.10	651.31	2.74
SgreTa0002155	Uncharacterized serine protease inhibitor	serine protease inhibitor	x		33.83	646.73	19.12
SgreTa0014303	x				176.21	645.78	3.66
SgreTa0017577	Aquaporin	water channel			0.39	635.34	1638.96
SgreTa0013377	Phosphoenolpyruvate carboxykinase [GTP]	gluconeogenesis			13.56	628.95	46.37
SgreTa0005752	Alpha-tocopherol transfer protein	intermembrane lipid transfer			12.98	594.56	45.79
SgreTa0014098	Phospholipase B-like	lipid degradation			206.76	577.99	2.80
SgreTa0000856	Transposase-like				25.93	576.67	22.24
SgreTa0008861	x				0.37	541.63	1456.67
SgreTa0017826	Sodium:neurotransmitter symporter	solute:sodium symport			0.49	540.53	1104.10
SgreTb0019287	x				3.11	528.47	169.79
SgreTa0015520	Protein yellow	melanization	x		2.75	520.09	189.08
SgreTb0006243	I-type lysozyme	anti-bacterial protein	x		16.96	519.35	30.62
SgreTa0009559	Gram-negative bacteria binding protein 3	pathogen recognition	x		15.40	510.04	33.13

[a] proteins related to immune response

[b] proteins that participate in larval moulting; some of them are known, other anticipated to digest cuticular chitin and protein (e.g., present in the MF)

Table 2. RNA-seq differential gene expression of cuticular chitin degrading enzymes in the highly secreting pleuropodia of *Schistocerca*.

(see below)

[a] upregulated (UP)/ downregulated (DOWN)

[b] the DEGs (781 upregulated) were ranked according to their RPKM in descending order, the number describes the position of the DEG in the ranked table; transcripts in bold were among the top 25% most abundant

[c] not applicable (expression low to undetectable in both samples, transcript filtered out)

[d] not significant

Family	Group	Protein	*Schistocerca* gene	UP/DOWN[a]	Fold change	Expression[b]
β-N-acetylhexosaminidase	I	NAG1	***Sg-nag1***	**UP**	**7.85**	**124 (15.88%)**
	II	NAG2	***Sg-nag2***	**UP**	**62.21**	**46 (5.89%)**
	III	Fused lobes	*Sg-fdl*	UP	14.18	592 (75.8%)
	IV	Hex	*Sg-hex*	UP	47.37	306 (39.18%)
chitinase	I-Major "moulting" chitinases	Chitinase 5	***Sg-cht5-1***	**UP**	**33.03**	**15 (1.92%)**
			Sg-cht5-2	UP	234.78	400 (51.21%)
	II-"Moulting" chitinases	Chitinase 10	*Sg-cht10-1*	na[c]		
			Sg-cht10-2	ns[d]		
	III-Cuticle assembly chitinases	Chitinase 7	*Sg-cht7-1*	ns		
			Sg-cht7-2	ns		
			Sg-cht7-3	ns		
	IV-Gut, fat body and other chitinases	Chitinase 8	*Sg-cht8-1*	na		
			Sg-cht8-2	na		
			Sg-cht8-3	na		
		Chitinase 6	*Sg-cht6-1*	ns		
			Sg-cht6-2	ns		
		Chitinase 2	***Sg-cht2***	**UP**	**2.81**	**188 (24.07%)**
	V-Imaginal disc growth factors	IDGF	*Sg-idgf-1*	UP	20.97	391 (50.06%)
			Sg-idgf-2	ns		
			Sg-idgf-3	ns		

1342

1343 **Table 3. MF proteases that were upregulated in the highly secreting**

1344 **pluropodia of *Schistocerca*.**

1345

MF protein[a]	Blast query[b]	*Schistocerca* transcript ID[c]	homolog/similar[d]	RPKM PLP	Fold change UP
Putative peptidase	D2KMR2	SgreTa0000627	similar	131.75	3.14
Aminopeptidase N-12	I3VR83	SgreTb0018983	similar	35.86	4.35
Neutral endopeptidase 24.11	Q9BLH1	**SgreTa0002467**	similar	2282.01	36.66
	Q9BLH1	SgreTa0017692	similar	133.30	240.28
	Q9BLH1	SgreTb0039123	similar	219.35	186.96
Ecdysteroid-inducible angiotensin-converting enzyme	Q9NDS8	**SgreTa0014009**	similar	1457.47	22.16
	Q9NDS8	SgreTa0017728	similar	62.71	57.08
Carboxypeptidase E-like	H9IST0	SgreTa0000925	homolog	139.81	10.95
Angiotensin-converting enzyme-like	H9IZ41	SgreTa0003298	homolog	23.64	5.65
Aminopeptidase N-like	H9JEW9	SgreTa0017219	homolog	391.03	437.93
Digestive cysteine protease 1, cathepsin L	H9JHZ1	SgreTa0000627	homolog	131.75	3.14
Serine carboxypeptidase	H9J242	**SgreTa0017657**	homolog	904.26	391.60
Serine protease HP21 precursor	H9JJA9	SgreTa0017649	similar	179.69	24.45
Trypsin-like serine protease - fibroin heavy chain	H9JPA8	**SgreTa0001636**	homolog	7578.31	153.48
Serine protease, Easter-like	Q2VG86	SgreTa0003188	homolog	485.97	837.45
	Q2VG86	**SgreTa0003661**	homolog	1332.79	45.18
	Q2VG86	SgreTa0006780	homolog	103.37	14.76

	Q2VG86	SgreTa0007424	homolog	29.62	79.13
	Q2VG86	SgreTa0007425	homolog	123.69	72.31
	Q2VG86	SgreTb0037249	homolog	21.76	249.74
	Q2VG86	SgreTb0039879	homolog	305.63	544.04
	H9JLZ4	SgreTa0010219	similar	46.12	20.75
	H9JLZ4	SgreTb0039024	similar	11.71	22.11
Serine protease 1	H9JXY6	**SgreTb0003860**	homolog	1727.41	22.31
Serine protease, Snake-like	H9IWW2	**SgreTa0000783**	similar	917.47	213.59

[a] proteomic sequencing of MF of the lepidopteran *Bombyx mori* (Zhang et al., 2014; Liu et al., 2018)

[b] Uniprot ID for blast on *Schistocerca* transcriptome

[c] transcripts in bold were among the top ten percent most highly "expressed" upregulated DEGs (Table 1)

[d] considered as homologous, if reciprocal blast retrieved the query sequence

Table 4. RNA-seq differential gene expression of *Schistocerca* lysozymes in the highly secreting pleuropodia.

Lysozyme type	Gene	UP/DOWN[a]	Fold change	Expression[b]
C-type lysozyme	***Sg-LyzC-1***	**UP**	**336.64**	**2 (0.26%)**
	Sg-LyzC-2	**UP**	**134.71**	**37 (4.74%)**
I-type lysozyme	***Sg-LyzI-1***	**UP**	**550.26**	**7 (0.90%)**
	Sg-LyzI-2	ns[c]		
	Sg-LyzI-3	**UP**	**30.62**	**76 (9.73%)**
	Sg-LyzI-4	DOWN	-34.41	1251 (81.50%)
	Sg-LyzI-5	ns		
Lysozyme-like	***Sg-Lyz-like-1***	**UP**	**192.68**	**150 (19.21%)**
	Sg-Lyz-like-2	ns		

[a] upregulated (UP)/ downregulated (DOWN)

[b] the DEGs (781 upregulated) were ranked according to their RPKM in descending order, the number (percentage) describes the position of the DEG in the ranked table; transcripts in bold were among the top 25% most abundant

[c] not significant

Table 5. RNA-seq differential gene expression of *Schistocerca* ecdysone biosynthesis enzymes in the highly secreting pleuropodia.

Gene	UP/DOWN[a]	Fold change	Expression[b]
shade (shd), Cyp314A1	ns[c]		
shadow (sad), Cyp315A1	ns		
disembodied (dib), Cyp302A1	UP	5.71	431 (55%)
phantom (phm), Cyp306A1	ns		
shroud (sro)	ns		
spook (spo), Cyp307A1	DOWN	-12.32	1368 (89%)
spook-like	ns		
neverland (nvd)	ns		
Cyp6t3	not found		
Cyp6u1	na[d]		
Cyp303a1	ns		

[a] upregulated (UP)/ downregulated (DOWN)

[b] the DEGs (781 upregulated and 1535 downregulated) were ranked according to their RPKM in descending order, the number (percentage) describes the position of the DEG in the ranked table

[c] not significant

[d] not applicable (expression low to undetectable in both samples, transcript filtered out)